

## Self-Assembling Peptide EAK16 and RADA16 Nanofiber Scaffold Hydrogel

Febrizio Gelain,<sup>\*,†</sup> Zhongli Luo,<sup>\*,†</sup> and Shuguang Zhang<sup>\*</sup>



Cite This: *Chem. Rev.* 2020, 120, 13434–13460



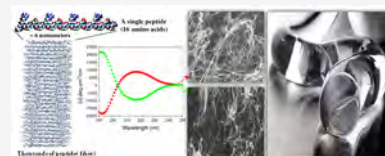
Read Online

ACCESS |

Metrics & More

Article Recommendations

**ABSTRACT:** Short peptides are ubiquitous in nature. They are found as hormones, pheromones, antibacterial and antifungal agents in innate immunity systems, toxins, and pesticides. But no one seriously considered that peptides could be useful as scaffold hydrogel materials. There has been a significant change since 1990 after the discovery of an ionic self-complementary peptide as a very interesting repeating segment in a yeast protein. It is now recognized that self-assembling peptides made from 20 natural amino acids have real material properties. Currently, many diverse applications have been developed from these simple and designer self-assembling peptide scaffold hydrogels and are commercially available. Examples include: (1) real 3D tissue cell cultures of diverse tissue cells and various stem cells, (2) reparative and regenerative medicine as well as tissue engineering, (3) 3D tissue printing, (4) sustained releases of small molecules, growth factors, and monoclonal antibodies, and (5) accelerated wound healings of skin and diabetic ulcers as well as instant hemostatic applications in surgery. Self-assembling peptide nanobiotechnology will likely continue to expand in many directions in the coming years.



### CONTENTS

1. Introduction	13435	5.2.1. 3D Niches for Stem Cell Culturing and Differentiation	13446
2. Structures of Self-Assembling Peptide Materials	13435	5.2.2. Ischemic Heart Disease (IHD)	13448
2.1. The Building Motifs of Self-Assembling Peptides	13435	5.2.3. Cartilage	13448
2.2. Structural Compatibility and Chemical Complementary Strategies of the Design Principle	13435	5.2.4. Bone	13449
3. Fine-Tuning the Design of Self-Assembling Peptide Materials	13437	5.3. Self-Assembling Peptide Materials in Nervous Regeneration	13449
3.1. Biomimetic Multifunctionalization	13438	5.3.1. Spinal Cord Injury Repair	13449
3.1.1. Functionalization Strategies	13438	5.3.2. Stroke	13450
3.1.2. Functional Motif Selection	13439	5.3.3. Peripheral Nerve Transections (PNT)	13451
3.1.3. Limitations of Self-Assembling Peptide Functionalization	13439	5.4. Anticipated and Unanticipated Uses of Self-Assembling Peptide Materials	13451
3.2. Tuning Biomechanical Properties	13439	5.5. Self-Assembling Peptide Materials and Technology Used in Clinic Areas	13452
3.2.1. Concentration and Sequence Dependence	13440	6. Concluding Remarks and Perspectives	13452
3.2.2. Branched Self-Assembling Peptides	13440	Appendix A	13452
3.2.3. Cross-Linked Self-Assembling Peptides	13442	Author Information	13453
4. Processing of Self-Assembling Peptides	13442	Corresponding Authors	13453
4.1. Electrospinning of Self-Assembling Peptides	13443	Author Contributions	13453
4.2. 3D Printing of Self-Assembling Peptides	13443	Notes	13453
5. Applications of Self-Assembling Peptide Materials	13445	Biographies	13453
5.1. Self-Assembling Peptide Materials in Controlled and Sustained Molecular Releases	13446	Acknowledgments	13454
5.2. Self-Assembling Peptide Materials in Tissue Repair	13446	Abbreviations	13454

Received: July 2, 2020

Published: November 20, 2020



1. INTRODUCTION

It has been known for decades that poly-L-lysine forms  $\alpha$ -helices at 4 °C and  $\beta$ -sheets at 50 °C, and under pH changes and in different solvents it also exhibits different structures with higher molecular weight.<sup>1</sup> Likewise, many alternating polypeptides, including (Glu-Ala)<sub>n</sub>, (Val-Lys)<sub>n</sub>, and (Lys-Tyr)<sub>n</sub>, form  $\beta$ -sheet structures with high molecular weight under certain conditions,<sup>2–5</sup> but it was not recognized that these polypeptides could form stable materials. It was known that glycinamide under repeated heating and cooling cycles will condense into some aggregates,<sup>6</sup> and by 1985 researchers used gamma irradiation to cross-link polypeptide (GVGVP)<sub>n</sub> into materials.<sup>7</sup>

The discovery of the first self-assembling peptide (SAP) in a yeast protein *Zuotin* was made in 1990 in researching Z-DNA-binding proteins.<sup>8</sup> Since the initial report in 1993,<sup>9</sup> the field of SAPs has expanded in many directions.<sup>10–55</sup> Useful SAP-based products in various areas include 3D tissue cell cultures, coatings, color dyes, semiconducting, and various hydrogels for tissue repair, tissue engineering, and materials for sustained molecular release. We do not attempt to exhaustively summarize the entire field in this review. To gain a broad understanding and a comprehensive view, interested readers should consult previous reviews and original literature.<sup>56–68</sup>

We here provide a timeline, from our point of view, to outline the significant advances in the field of SAP scaffold materials (Figure 1 and Appendix). We focus this review on SAP nanofiber hydrogel materials, particularly RADA16- and EAK16-derived SAPs, and their various uses: this is because they are the most widely used SAPs in basic research, preclinical research, and clinical applications.

We would like to emphasize that this review is focused only on short designed peptides. Protein-based hydrogels (>40 residues) is itself an actively pursued field not covered here. Interested readers should consult the literature to gain more understanding.<sup>69–78</sup>

2. STRUCTURES OF SELF-ASSEMBLING PEPTIDE MATERIALS

There are several kinds of self-assembling peptide hydrogels, including three-stranded collagen helices and  $\beta$  hairpins, but  $\beta$ -sheet and  $\alpha$ -helix SAP hydrogels predominate (Figure 2).  $\beta$ -Peptide materials usually comprise several to tens of amino acids but can be as short as 2–3 amino acids,<sup>35,59,60</sup> On the other

hand,  $\alpha$ -helix peptides are usually greater than 10 amino acids. The formation of  $\alpha$ -helix peptide-based hydrogels usually require ~20 residues.<sup>15,18,20,30,45,46,50</sup> Both types of SAP hydrogels form well-ordered nanostructures. Most commonly, variations of nanofibers form ordered networks that assemble into highly organized scaffolds. These retain extremely large amounts of water molecules as hydrogels with very high-water content (~99%, from 3 to 10 mg/mL peptide). Such SAP hydrogels have found diverse uses.<sup>9–13,64–68</sup> It is possible to produce many kinds of SAPs, either through systematic designs or combinatorial library selections.<sup>49,57–68</sup>

2.1. The Building Motifs of Self-Assembling Peptides

The first naturally occurring SAP is EAK16, with a unique repetitious segment (AEAEAKAKAEAEAKAK) in a natural yeast protein.<sup>8,9</sup> This and the designed variant RADA16 (RADARADARADA)<sup>13</sup> were synthesized using natural L-amino acids by solid-phase chemistry, and later, using D-amino acids to design the chiral D-SAPs,<sup>28,29</sup> noting that chiral D-peptides are resistant to L-protease degradation (Figure 3). L-Form SAPs including EAK16 and RADA16 and their D-form analogues show inverted CD spectra in stable  $\beta$ -sheet in physiological solution.<sup>28</sup> The peptide hydrogels are made of various building motifs with secondary structures that can be regulated by (i) amino acid sequences, (ii) peptide concentration, (iii) pH value, (iv) temperature, and (v) the medium ionic composition. These conditions can significantly influence the dynamic peptide structures as well as the self-assembly process.

Some peptides have dynamic secondary structures. EAK12-d and DAR16-IV\* change from  $\beta$ -sheet to  $\alpha$ -helix with a temperature change from 60 to 90 °C. The conformation change can be regulated by pH changes.<sup>79,80</sup>

2.2. Structural Compatibility and Chemical Complementary Strategies of the Design Principle

The designs of chiral SAP need to consider: (1) the primary structure with structural compatibility and chemical complementary (+ and – charges, hydrogen bond formations), and (2) molecular properties of the individual amino acid.

Self-assembling peptides design may rely on: (i) alternating hydrophobic and hydrophilic sides, (ii) alternating positively charged and negatively charged residues, (iii) using natural chiral L- or unnatural D-amino acids, and (iv) polar and nonpolar activity. Once formed, the designer peptide units undergo self-assembly to become an integral part of the desired material structure with defined functions. The SAP material may include multi bioactive motifs in a suitable microenvironment.

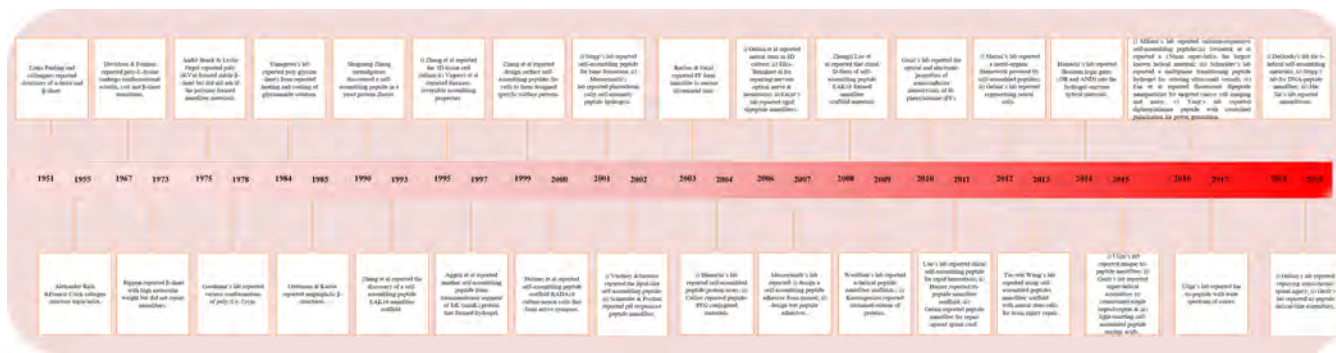
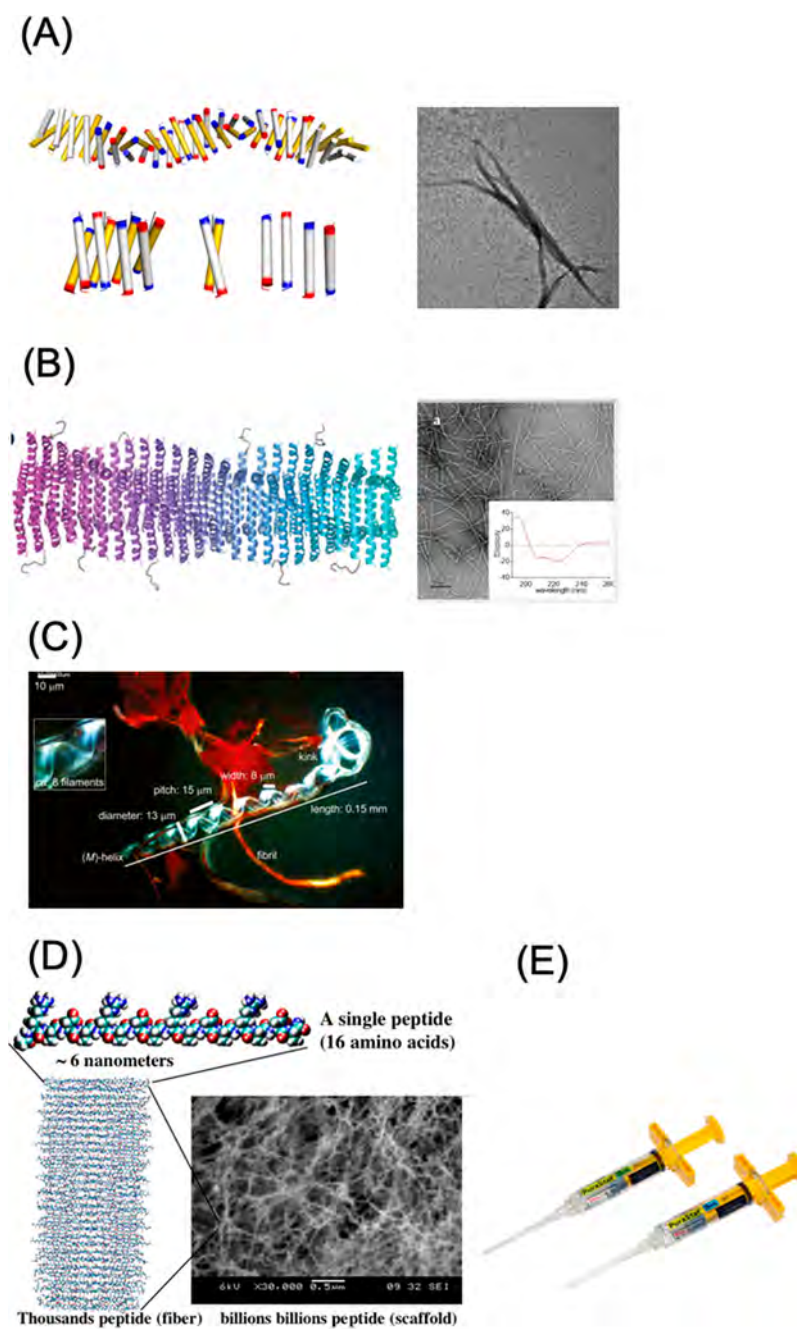
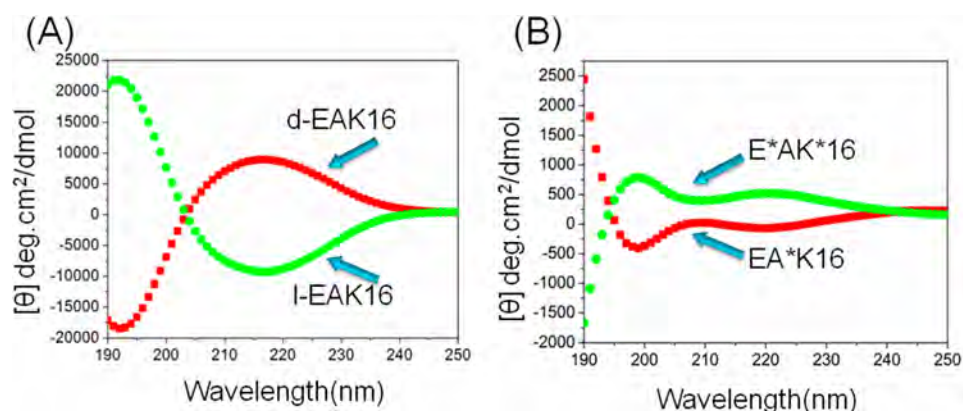


Figure 1. Timeline of the significant discoveries in the field of various self-assembling peptides. For clarity and readability, a list with the identical information for clear reading is at the end as an Appendix.



**Figure 2.**  $\alpha$ -Helical and  $\beta$ -sheet SAP nanofiber hydrogel materials. (A) (left panel) The superhelical repeat consists of 16 dimers of  $\alpha$ -helices, which are colored blue and red at the N- and C-termini, respectively. The white and yellow rods represent two identical helices that form homodimers. The  $\alpha$ -helix dimer subunits progress perpendicularly to the superhelical axis. The basic unit of the whole amyloid-like assembly is a pseudo-2-fold symmetric cross-strand parallel helix dimer, with 2-fold rotational axis. In each sheet, there are two different types of 2-fold symmetric antiparallel  $\alpha$ -helix pairs. (right panel) TEM image of superhelical composed numerous  $\alpha$ -helix pairs. Image courtesy of S. Q. Zhang and W. DeGrado, Reproduced with permission from ref 50. Copyright 2018 Springer-Nature Publishing. (B) (left panel) Right-handed superhelix nanofibers composed of numerous  $\alpha$  helix pairs. (right panel) The TEM image of nanofiber hydrogel assembled from the superhelices, an  $\alpha$  helix CD spectrum is in the inset. Image courtesy of J. Collier. Reproduced with permission from ref 228. Copyright 2017 ACS Publishing. (C) Optical microscopy under polarized light of Congo-red-stained assemblies of the peptide H-(Val-Ala-Leu)<sub>4</sub>-OH. This left-handed superhelix material was obtained after a 14-day incubation. The insert of one enlarged helix pitch shows the filaments of which the twisted tape is composed. Image of courtesy of D. Seebach. Reproduced with permission from ref 45. Copyright 2016 Wiley-VHCA AG, Zurich. (D) Self-assembling peptide RADA16 nanofiber scaffold that forms hydrogel. Amino acid sequence of RADA16-I, molecular model of a single RADA16-I peptide. The calculated peptide dimensions are approximately 6 nm long depending on end-capping, 1.3 nm wide and 0.8 nm thick; billions of individual peptides self-assemble into a nanofiber depending on the fiber length as revealed by the SEM image of RADA16-I nanofiber scaffold. Scale bar = 0.5  $\mu$ m. RADA16-I peptide forms nanofibers in aqueous solution that further form hydrogel with extremely high-water content (99.5–99.9% w/v water). (E) Image of RADA16-I scaffold hydrogel filled in 3 and 5 mL syringes. Reproduced with permission from 3D-Matrix, Ltd., Tokyo, Japan, Copyright 2020.



**Figure 3.** Circular dichroism (CD) spectra of the peptides at 37 °C. (A) Pair of d-EAK16 and l-EAK16; the l-EAK16 spectrum is the lower part and d-EAK16 spectrum is the upper part. (B) Pair of EA\*K16 and E\*AK\*16; EA\*K16 spectrum is the lower part and E\*AK\*16 spectrum is the upper part. The four peptides showed stable secondary structures at the 37 °C. Note the completely inverted CD spectra based on chirality difference. D-SAP first reported from ref 28. Reproduced with permission from ref 229. Copyright 2011 Biomaterials, Elsevier.

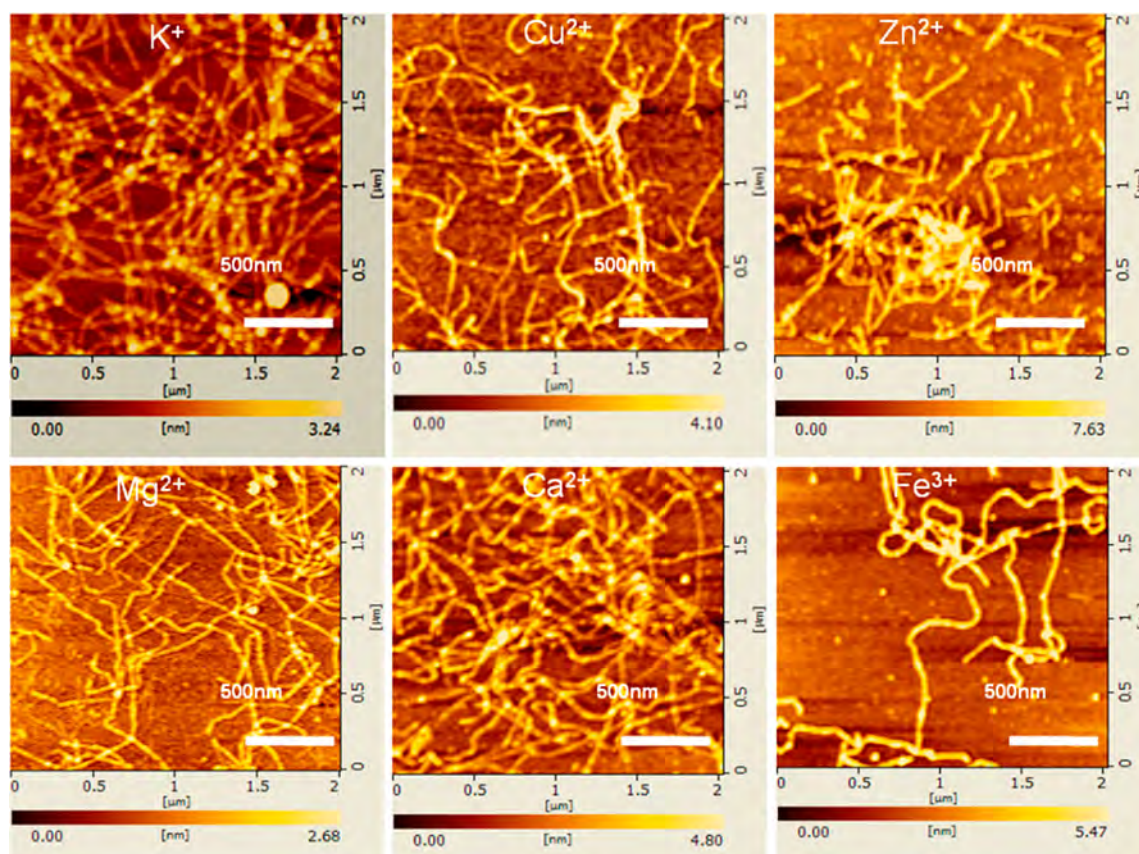


**Figure 4.** AFM images of the SAP. Various metal ions influence peptide self-assembly. d-EAK16 was incubated in various ionic solutions: K<sup>+</sup>, Cu<sup>2+</sup>, Zn<sup>2+</sup>, Mg<sup>2+</sup>, Ca<sup>2+</sup>, and Fe<sup>3+</sup> (10 mM each). These metal ions influence the peptide self-assembly to different degrees. Reproduced with permission from ref 229. Copyright 2011 Biomaterials, Elsevier.

### 3. FINE-TUNING THE DESIGN OF SELF-ASSEMBLING PEPTIDE MATERIALS

Almost all self-assembling peptides are able to retain an enormous amount of water to form various hydrogels because of their alternating hydrophilic and hydrophobic amino acid residues. Hydrophilic residue side chains can interact with water directly, and water molecules form clathrates to surround hydrophobic residue side chains. For any given peptide, if there are too many hydrophobic residues, the peptide would become water-insoluble and precipitate out of water. On the other hand,

if there are too many hydrophilic residues, the peptide will be highly water-soluble, thus the hydrogel is unable to form. The peptide molecules can be induced to self-assemble into ordered-nanostructure materials such as nanofibers, nanotubes, and nanovesicles. The formation of ordered nanostructures and their mechanical properties are influenced by several factors: (i) amino acid sequence, (ii) chiral amino acid arrangement, (iii) length of the peptides, (iv) peptide concentration, (v) self-assembling time, (vi) the level of hydrophobicity residues, and (vii) various ions (Figure 4). For example, the hydrophobic

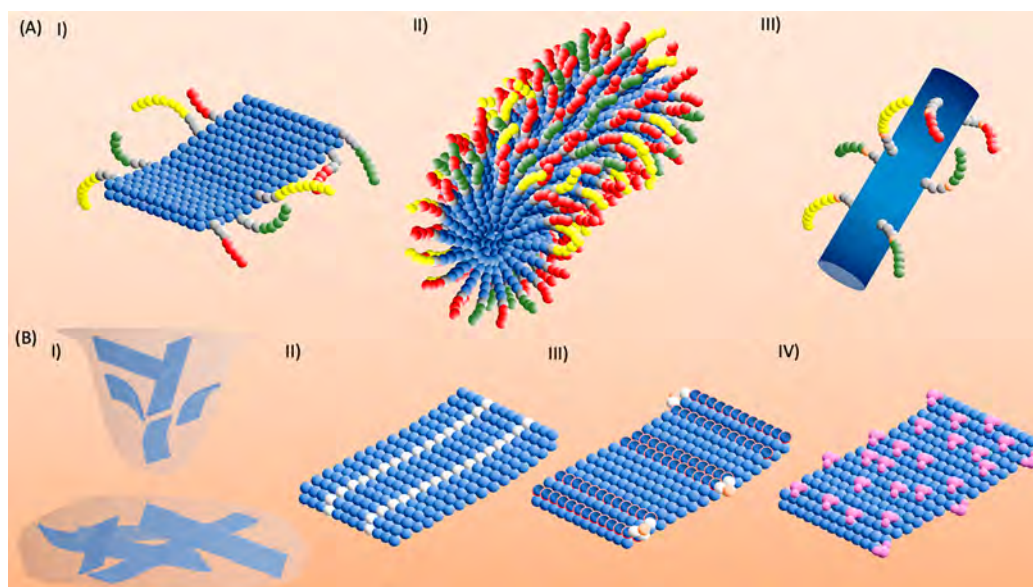


**Figure 5.** Self-assembling peptides fine-tuned designs. Self-assembling backbones are colored in blue. Spacers and hydrophobic residues are marked in white, unnatural residues are pink. Different functional motifs are yellow, red, and green. (A) Most common strategies of SAP functionalization (white dots = linker amino acids, blue dots = backbone amino acids, other colors = active motifs) (I) RADA-like SAPs, forming cross- $\beta$  structures, can be sequence-extended at one or both termini with a Gly-spacer and functional motifs of different length and bioactivity. (II) In PAs, functional motifs take an active part in self-assembling, dictating nanostructure morphology, and kinetics. Spacers between functional motifs and self-assembling backbone are not usually used except for a charged residue improving PA solubility. Various functional motifs can be mixed within the same self-assembled hydrogel, but the ranges of length and net-charge available for functionalization are more limited in this case. (III) SAPs featuring different self-assembled nanostructures (generic self-assembled core) can be extended with Gly-spacers and unnatural residues featuring a click-reactive group (e.g., *O*-propargyl serine) available for binding after self-assembling in order not to perturb the standard SAP self-aggregation. Different azide-containing functional motifs can be later click-linked in mild-reactive conditions. (B) Tuning of SAP mechanical properties. (I) By increasing SAP concentration, it is possible to raise the density of transient noncovalent interactions among self-assembled nanostructures. (II) Alternatively, punctual mutations in the self-assembling backbone with hydrophobic residues can tighten hydrophobic interactions. (III) Branched-SAPs, usually comprising a double-Fmoc Lys, equally spaced with glycines in all branches (for appropriate solubility and flexibility), should share the same self-assembling backbone of the linear counterpart (circled residues) so as to favor their own chains integration. Linear and branched-SAPs are mixed before self-assembling to warrant appropriate uniform distribution. (IV) Cross-linking, with both natural and synthetic cross-linkers (violet particles), acts at longer time scales than self-assembling phenomenon, therefore it mainly tightens already assembled SAP nanostructures.

residues, Ala, Val, Ile, Leu, Tyr, Phe, and Trp can significantly influence the mechanical properties of the structure and the speed of their self-assembly.<sup>81–83</sup>

Given the broad variety of potentially available self-assembled nanostructures and recent advances in peptide synthesis technology,<sup>84,85</sup> SAP hydrogels show various options for customization for a specific application. While maintaining the same self-assembling strategy, several modifications including punctual sequence variations, backbone chain extensions, chemical, or physical linking are just a few of the available possibilities.<sup>66</sup>

### 3.1. Biomimetic Multifunctionalization

Self-assembling peptides can be tailor-made so as to intimately interact with cells, cytokines, and tissues where they are implanted. This is the principle underlying biomimetic materials. Most of the proteins composing the extracellular matrix (ECM) display a number of bioactive sites that are made of peptides and/or sugars available for cellular binding, internalization, and regulating their homeostasis. Biofunctionalization of some biomaterials may require the development of *ad hoc* chemical reactions for each new functional motif, whereas the biofunctions of SAPs can be designed from the beginning at the single amino acid level.

**3.1.1. Functionalization Strategies.** SAPs feature the unique advantage of sharing the intrinsic chemical composition of most functional motifs, thus paving the way for their

functionalization by using the same synthesis technique. In most cases, cross- $\beta$ -forming SAP functionalization is achieved by simply extending the original peptide sequence, normally at the C-terminus (providing for fewer synthesis errors), with functional motifs eventually interspaced via a glycine spacer favoring flexibility and exposure for motif binding with cell membrane adhesion proteins<sup>23</sup> but also providing a backbone chain stabilization in self-assembled cross- $\beta$  structures.<sup>86</sup> There is virtually no limit to the number of possible functional motifs that can be added to a strong self-assembling backbone. A number of differently functionalized SAPs, sharing the same self-assembling sequence, can be mixed together prior to gelation and, upon exposure to a stimulus triggering self-assembly, provide a nanostructured scaffold displaying multiple functional motifs. By this simple strategy, it is feasible to customize, in terms of bioactivity, an SAP scaffold hydrogel for each new application in regenerative medicine.

In the example of the chimeric lipid–peptide amphiphile (PA),<sup>14</sup> the functional motif is located at the C-terminal segment, close by the  $\beta$ -structural forming section, thus shortening the total length. It also influences the gelation kinetics and morphological topography at the nanoscale.<sup>87</sup> Moreover, bio-orthogonal chemical reactions may be used to enable click-chemistry functionalization of self-assembled nanofibers from modified SAPs containing azides and alkenes after self-assembling. By changing the amount and type of peptide

decoration, it is also possible to control the density of functional motifs and multifunctionalization, respectively<sup>88,89</sup> (Figure 5A).

**3.1.2. Functional Motif Selection.** Finding the right functional motifs is one of the most important aspects of SAP nanobiotechnology. They can be obtained from a rich literature on various motifs: (a) through protein docking analysis *in silico*, (b) through screening of synthesized peptide libraries, and (c) via phage display panning against a specific target (e.g., cell, drug).<sup>90,91</sup> RGD from fibronectin and IKVAV from laminin are the most used functional motifs in SAP applications because of their short length, easy synthesis, and ubiquitous distribution in the ECM of living tissues.<sup>14,92–94</sup> A plethora of different functional epitopes from other ECM components, e.g., collagens, hyaluronic acid, and osteopontin,<sup>92,95–97</sup> have been widely used with SAPs, but they also comprise binding sites of cytokines, e.g., TGF- $\beta$ <sup>1</sup><sup>98</sup> or mimics/binding sites of transmembrane proteins, e.g., N-cadherin/Notch, respectively.<sup>99–101</sup> Functional motifs can also be computationally or empirically designed to selectively bind just specific targets such as viruses<sup>91</sup> and tumor cells.<sup>102</sup>

Notwithstanding the above, the most powerful technique for the discovery of novel functional motifs particularly fitting the SAP technology potential is phage display. Phage display is a rather easy and useful technique for the identification of peptides binding a specific target, either a protein, a cell, or an inorganic material.<sup>90</sup> It makes use of genetically modified bacteriophages displaying peptides fused to the N-terminal of their outer proteinaceous capsid. Libraries can display up to  $10^8$ – $10^{10}$  different combinations of peptides (commercial libraries provide 7- or 12-residue exposed peptides) coded in the bacteriophage genome. After a subsequent round of panning against the target, it is possible to select phages, namely, those with the functional motifs most efficiently bound to it. Compared to other techniques, phage display can be a fast process and can be applied to structurally complex biological targets at almost physiological condition. It has been heavily used in biopharma. Nonetheless, the selection of a specific binding motif does not end with its identification but, depending on the scope of the research, may require additional efforts to understand the actual bioactivity and potential side effects.

One of us (Gelain and colleagues) used phage display in work on neural stem cells and spinal cord regeneration.<sup>103</sup> A bone marrow homing motif 1 (BMHP1) coupled directly to peptide (RADA)<sub>4</sub> and assembled into a peptide nanofiber hydrogel achieved efficient differentiation of neural stem cells (NSCs) in 3D tissue culture without additional coating additive.<sup>23</sup> The same BMHP1 motif was later used as a self-assembling backbone of a novel and different class of biotinylated hierarchically SAPs.<sup>104</sup> Phage display was used to discover novel functional motifs including KLPGWSG, FAQRVPP binding to NSCs,<sup>105</sup> or differentiated neural stem cell progeny,<sup>37</sup> which were both shown, once linked as functional motifs to (LDLK)<sub>4</sub>, to favor adhesion, survival, neuronal differentiation of NSCs *in vitro*, and spinal cord regeneration *in vivo* in acute and subacute injuries.<sup>54</sup>

Sawada et al. selected via phage display a specific peptide sequence capable of detecting the self-assembled state of a  $\beta$ -sheet peptide Ac-YEYKYEYKYEY-NH<sub>2</sub>, binding to discrete sites on the assembled nanostructures. They conjugated the 11-residue peptide to an RGDS epitope to obtain the spontaneous high-density functionalization of the assembled scaffold, triggering adhesion of human cervical cancer cells *in vitro*.<sup>106</sup> Others couple phage-display-identified collagen-like functional motifs to peptide amphiphiles and through a self-templating

process they obtained controlled deposition of biomimetic nanostructures driving both spatial self-organization of cultured preosteoblasts and hydroxyapatite deposition *in vitro*.<sup>107</sup> Others used phage-display-derived peptides binding to graphite to study the differently self-organized nanostructures of an SAP in response to variations of the electrochemical bias.<sup>108</sup> Okuyr et al. reported the use of phage display to efficiently functionalize peptide amphiphile with a nerve growth factor NGF-binding motif, showing high peptide amphiphile affinity for NGF and capable of enhancing PC-12 cell differentiation *in vitro* by activating their NGF receptor-related pathways.<sup>109</sup>

**3.1.3. Limitations of Self-Assembling Peptide Functionalization.** Despite the considerable potential for SAP functionalization described in the previous subsection, various limits and strategies have to be carefully weighed when designing a biomimetic SAP as self-assembly is primarily the result of weak molecular interactions coming from both the self-assembling backbone and the functional motifs. The maximum length allowed for a functional motif, and as a consequence, of the entire SAP, may be restricted by technical limits coming from peptide synthesis technology, overall peptide solubility, or by the chosen self-assembling strategy. For example, in peptide amphiphiles, it is well-known that the length ratio between hydrophobic tails and hydrophilic heads may change the self-assembled nanostructures, nanotubes, nanorods, or nanovesicles. The distribution of hydrophilic and hydrophobic residues should be tailored so as to avoid hydrophobic patches, hampering peptide solubility, or causing fast random hydrophobic collapses competing with the expected ordered self-assembling. Alternatively, important clusters of hydrophilic residues may destabilize the assembled molecular structures.<sup>110</sup> The total net charge and charge distribution are both crucial for SAPs and CAPs, as electrostatic forces are usually the main driving energies triggered by the external stimuli triggering self-assembly.<sup>110,111</sup> As an example, in RADA-like SAPs, the isoelectric point of the functionalized peptide heavily influences its self-assembling status at a given pH, its viscosity and, consequently, its final biomechanical properties after self-assembling. Some functional motifs selected through phage display may be biologically active only if linked to the N-terminal of the SAP sequence. This must be verified and, in some SAPs, N-terminal functionalization may not be an available option.<sup>112</sup> The functional motif may unexpectedly feature a propensity to self-assemble by itself or with the remaining SAP sequence, competing with or altering the self-assembly propensity of the backbone sequence. Some of these hurdles can be efficiently addressed with an appropriate design through molecular dynamics or, empirically, by rational punctual mutations of the chosen functionalized SAPs or by interspersing self-assembling backbones and functional motifs with longer glycine-based spacers (Figure 6).<sup>86,110,112</sup>

### 3.2. Tuning Biomechanical Properties

When considering the regeneration of different tissues, or 3D tissue cell culture, it is widely recognized that the mechanical properties of the material play a crucial role.<sup>113,114</sup> For example, to promote scaffold-tissue integration, an implanted prosthesis should closely match the behavior of the tissues to be regenerated in stiffness and viscoelasticity, ranging from 100 Pa for solid-soft tissues, e.g., spinal cord,<sup>114</sup> to 25 GPa for hard ones, e.g., trabecular bone.<sup>115</sup> SAP biomechanics can have a dramatic effect on stem cell differentiation and survival *in vitro*.<sup>105,113,116</sup> It is therefore important to fine-tune the

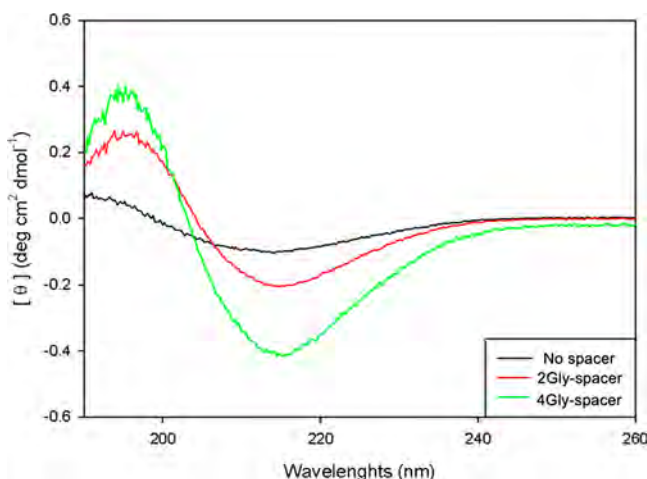


**Figure 6.** CD spectra of  $\beta$ -forming SAP extended with a variable-length Gly spacer and a 7-residue functional motif. Close proximity of functional motifs to the self-assembling backbone can significantly alter  $\beta$ -structures (CD spectra  $\sim 195$  nm and  $\sim 215$  nm), while increasing the number of Gly can exert a beneficial effect on the overall  $\beta$ -aggregation of the functionalized SAP.

biomechanical properties of the SAPs. The self-assembling phenomenon consists of a number of weak noncovalent interactions: (i) hydrogen bonding, (ii) aromatic stacking, (iii) electrostatic interactions, (iv) van der Waals interactions, and (v) hydrophobic interactions.<sup>117</sup> The self-assembled hydrogel is suited as a filler, lubricant, or weak construct for *in vitro* tissue cell culturing. Significant efforts have been focused on improving these intrinsic mechanical limitations.<sup>118,119</sup>

### 3.2.1. Concentration and Sequence Dependence.

Among the most helpful methods in fine-tuning the overall stiffness of SAP scaffolds, concentration plays a major role within a concentration range specific for each SAP sequence, usually ranging from its minimum concentration of assembly to its maximum solubility in water (Figure 5B). SAP's  $G'$  storage

modulus (pointing at its stiffness) varies proportionally along with the density of transient interactions among self-assembled nanostructures vs its concentration (Figure 7).<sup>111</sup> The main drawback to tuning via concentration is that it can influence the overall porosity of the assembled scaffold. In the case of 100% functionalized peptides, the high density of functional motifs influences the self-assembled nanostructures and availability for cell binding. These phenomena can influence the diffusion of cytokines<sup>120</sup> and/or the reaction of cells seeded within the scaffolds.

Moreover, in biomedical applications where a water-based solution is usually used, this range may be rather narrow, e.g., 0.5% to 3% w/v, yielding to  $G'$  values from few Pa to some KPa.<sup>111,121</sup> Another method is to fine-tune the overall hydrophobicity of the SAP, either the self-assembling backbone or the functional motif. Adding more hydrophobic residues may yield stiffer scaffolds.<sup>37,82,83,122</sup> Key considerations for biomimetic SAP design are listed in Table 1. Additional strategies including cross-linking are needed so as to further increase SAP scaffold stiffness with less hindrance of other important biomaterial properties.

**3.2.2. Branched Self-Assembling Peptides.** Branched-peptide synthesis can be easily achieved, among other ways, by using double-Fmoc-Lys residues followed by simultaneous coupling of two identical peptidic branches. Other methods leading to heterogeneous branching involve the use of differently protected Lys-residues or more sophisticated click-chemistry. Branching of SAPs has been used to increase the overall density of functional motifs or to allow for the exposure of multiple and/or different moieties available for cell binding.<sup>121</sup> Branched SAPs have also been used as “molecular connectors” of self-assembled nanostructures to obtain up to an 8-fold increase of SAP hydrogel stiffness.<sup>123,124</sup> The increase in stiffness was proportional to the number of branches featuring a self-assembling backbone capable of integrating with those of linear SAPs (*i.e.*, sharing the same self-assembling sequence and interspaced with the Lys-connector and Gly).

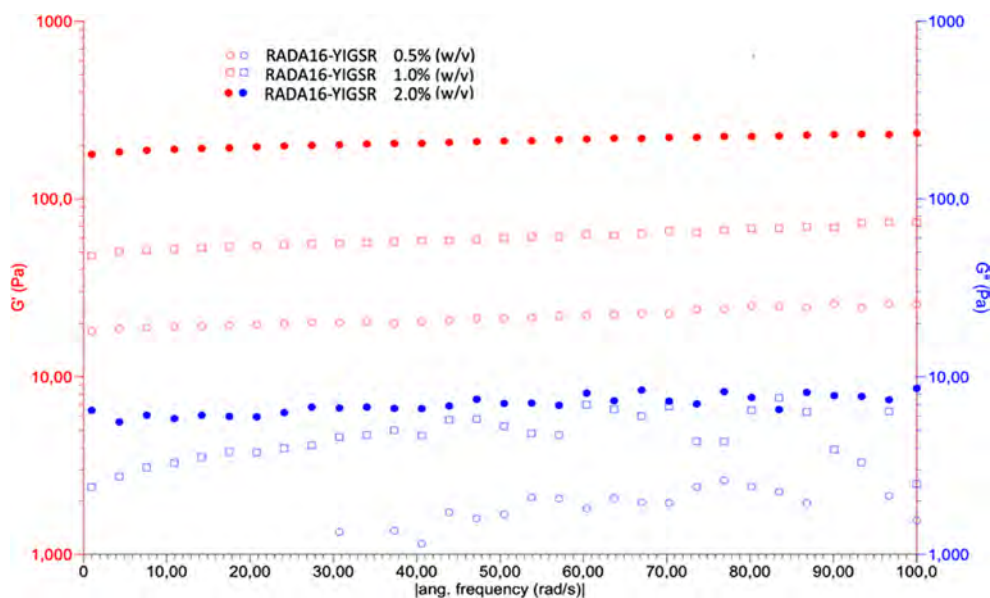


**Figure 7.** Frequency sweep test performed at a fixed angular oscillatory setup.  $G'$  and  $G''$  moduli of RADA16-YIGSR dissolved and assembled at different concentrations. By increasing the concentration from 0.5% to 2% (w/v), the storage modulus increases from  $\sim 20$  to  $\sim 200$  Pa. In general, further concentration increments should be carefully evaluated per each SAP sequence as solubility issues may arise.

Table 1. Key Considerations for Designs of Self-Assembling Peptides

key considerations	refs
The self-assembling backbone is the pivot of the overall scaffold, regulating the self-assembling propensity, its kinetics of assembly, and determining both secondary structure arrangements and the morphology of the assembled peptide nanostructure.	9–12,30,56–66
Functional motifs provide biological or nonbiological functions to SAPs. They can be binding sites for cytokines and/or cell transmembrane proteins, active/catalytic sites for enzymatic reactions, but also molecular beacons for DNA recognition and tags for scaffold tracking both <i>in vitro</i> and <i>in vivo</i> . Usually it is preferable not to have only the functional motifs undergo self-assembly. Unexpected interactions (both favorable and unfavorable) with the backbone self-assembly may occur.	37,39,66,105,110
Spacers can provide proper flexibility and exposure of the functional motifs from the self-assembling backbones. They can also decrease the influence of functional motifs over self-assembling backbone structures.	66,86
The overall increase in length of the functionalized SAP may decrease its solubility or alter the morphology of the self-assembled nanostructures.	66,86
Increasing the concentration of SAPs increases the viscosity and stiffness of peptide solutions and self-assembled SAP hydrogels respectively, but it can also decrease scaffold porosity or increase the spatial density of the exposed functional motif.	105,115
The isoelectric point of the SAP sequence (including both functional motif and self-assembling backbone) dictates the pH-threshold triggering its self-assembly and the proper ionic composition of the aqueous solvent used for its dissolution.	80,82,97
Punctual mutations of both the self-assembling backbone and the functional motifs favoring more hydrophobic residues may strengthen mechanical properties but can also affect SAP solubility and bioactivity of the functional motif.	41,82,83,112

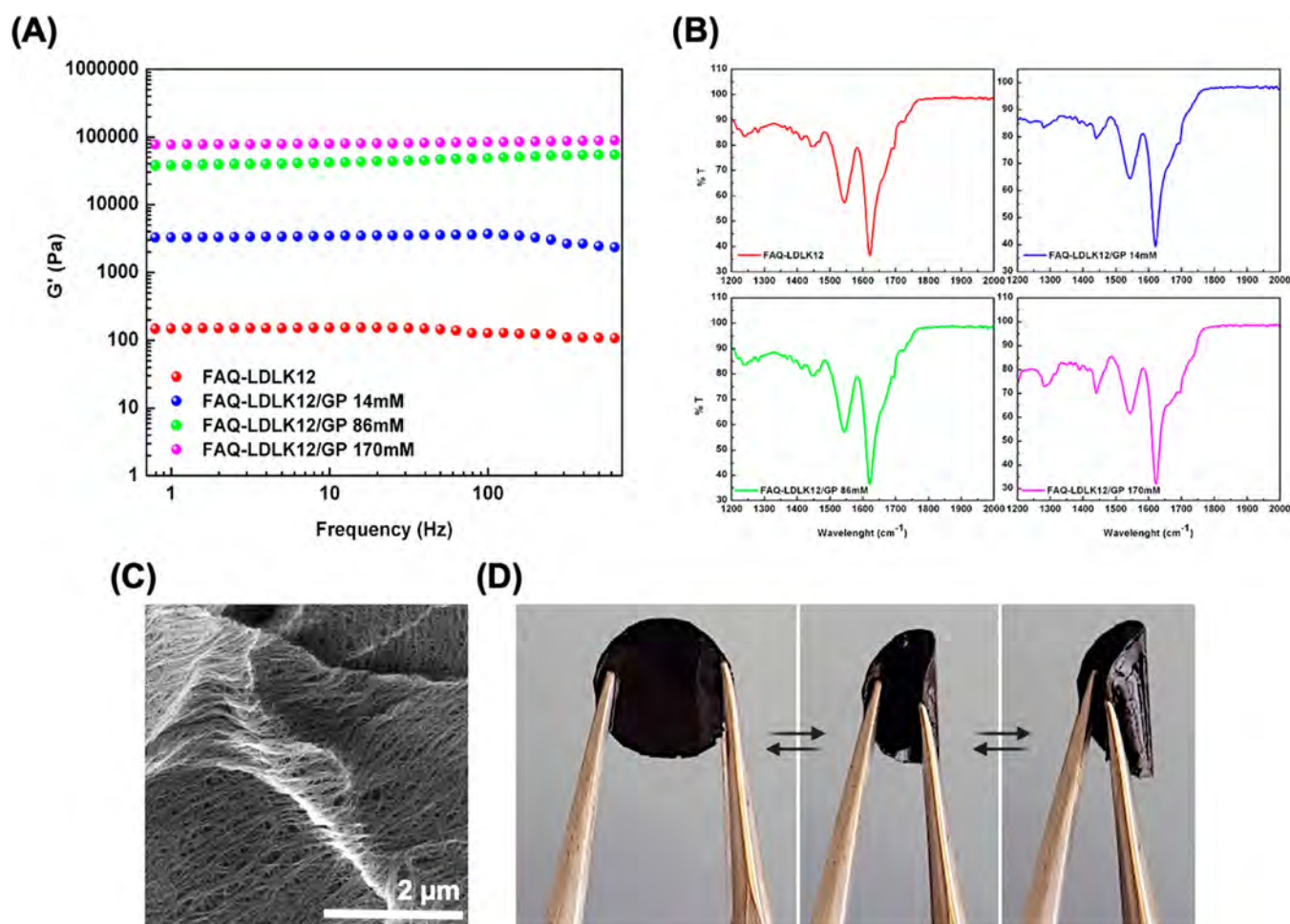


**Figure 8.** Biomechanics and  $\beta$ -structure formation of cross-linked LDLK12-based SAPs. (A) Storage modulus ( $G'$ ) increments of FAQ-LDLK12 SAP (5% w/v) along with increasing concentrations of genipin: red is for pure SAP. Cross-linked SAP hydrogels stiffness increased from 0.1 to 100 KPa (1000 $\times$ ). (B) FT-IR spectra of cross-linked SAPs in the amide I and amide II region showing the three major peaks at 1695, 1630, and 1540  $\text{cm}^{-1}$  confirm the cross- $\beta$  structuration of both standard and cross-linked SAPs. (C) SEM image of the cross-linked SAP showing long, aligned, and entangled nanofibers. (D) Photographs of a flexible cross-linked SAP membrane resilient to compression. Reproduced with permission from ref 119. Copyright 2018 The Royal Society of Chemistry. Images (A), (B) and (C) are courtesy of Raffaele Pugliese.

The increase in stiffness also correlates well with increases in the fraction of  $\beta$ -sheet arrangements of the chosen SAPs. Coarse-grained molecular dynamics demonstrated that branched SAPs well-integrated within the self-assembled standard cross- $\beta$  structures of (LDLK)<sub>12</sub> act as “fasteners” of the formed nanostructures and do not hamper the linear SAP

self-assembling propensity. The main advantages of this modular approach are (i) the minimal amount of the branched-SAPs necessary to exert the maximum  $G'$  increments (1:500 molar ratio against linear SAPs), (ii) the directly proportional correlation between stiffness and number of self-assembling backbone branches leaving the door open for further



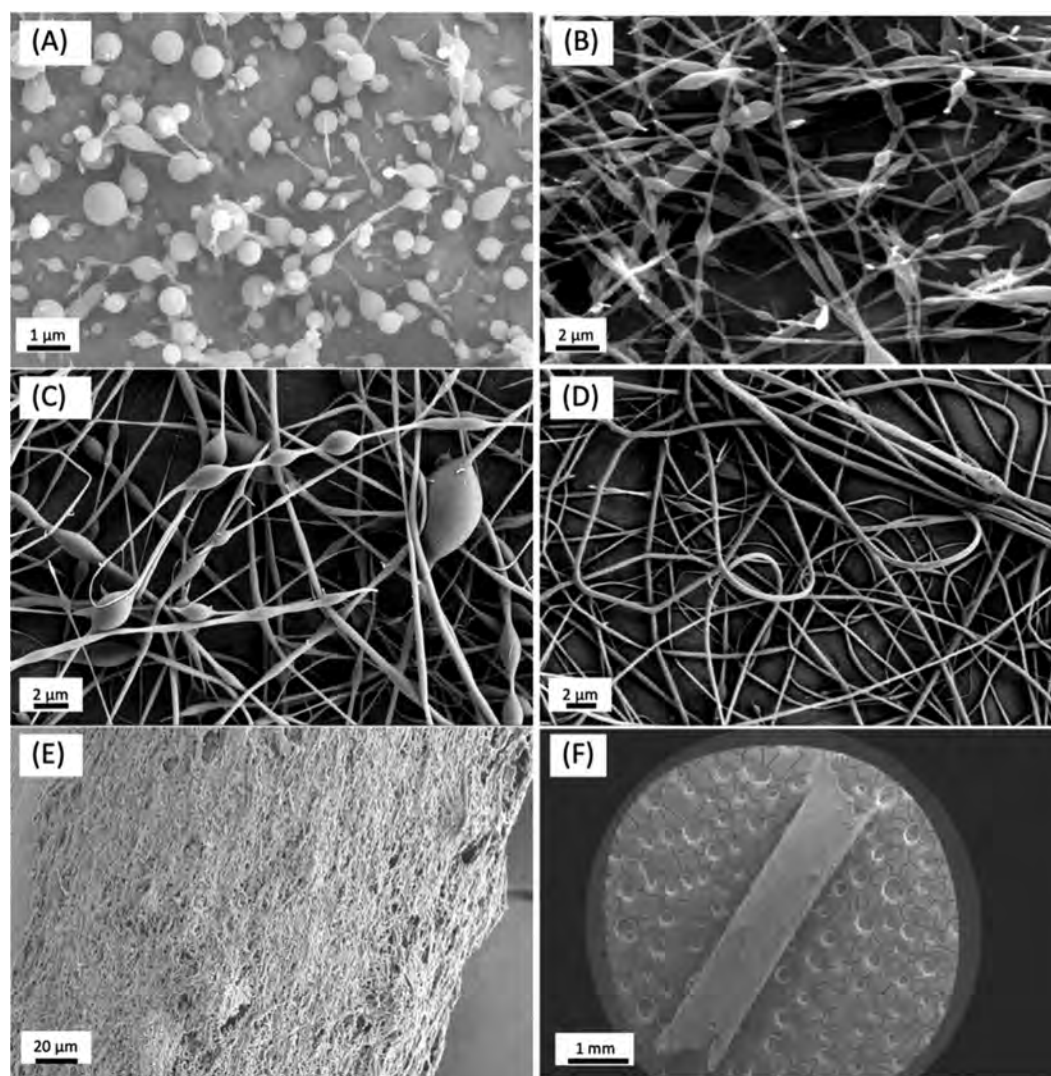


**Figure 9.** FE-SEM micrographs of electrospun SAPs. (A) SAP solution with low concentration (10–15% w/v) forms nanoparticles and very thin fibers with numerous beads. (B) At higher concentration (15–20% w/v), fibers are thin with numerous round and spindle shape beads. (C) By further increasing the SAP solution concentration (20–30% w/v), thicker fibers with few spindle-shaped beads appear. (D) Finally, with optimal high-concentration (30–40% w/v), fibers are thick, uniform, and defect-free. Electrospun microchannel wall details are depicted in (E). (F) A defect-free electrospun microchannel suited for nervous regeneration is well formed (image courtesy of Mahdi Forouharshad).

amelioration, (iii) the possibility of tuning hydrogel biomechanics without altering porosity, the functional motif density, or linear SAP sequences, and (iv) the absence of any potentially harmful cross-linking reaction.<sup>123</sup> Nonetheless, if compared to the wide range of stiffnesses found in living tissues, this approach still lacks the range of stiffness properties (maximum increment was up to 8 KPa) required by many tissue engineering applications.

**3.2.3. Cross-Linked Self-Assembling Peptides.** Over the past few years, it became more evident that covalent linking has become necessary to achieve more substantial improvements of the mechanical properties of peptides assembled usually through weak interactions. Collagen, chitosan, gelatin, and cellulose biomaterials have been successfully cross-linked to improve their biostability and biomechanics *in vitro* and *in vivo*,<sup>125,126</sup> using both synthetic and natural cross-linkers.<sup>126,127</sup> Genipin, a homobifunctional naturally derived cross-linker, was used to enhance the mechanical properties of a Fmoc-tripeptide hydrogel to be used as a drug delivery system<sup>128</sup> but also with a functionalized (LDLK)<sub>4</sub>-based SAP.<sup>123</sup> Genipin, extracted

from *Gardenia jasminoides* fruits and commonly used in Chinese medicine, is purportedly thousands of times less toxic than glutaraldehyde. It reacts with primary amines and is capable of bringing the  $G'$  and mechanical stress failure of the tested SAP up from 0.7 to 110 KPa (157 $\times$ ), and from 39 to 2576 Pa (66 $\times$ ), respectively (Figure 8). Such a significant change in the hydrogel properties is proportional to the dose and exposure time of genipin, mirrored by backbone primary amine involvement in the cross-linking reaction and increased (more than 2-fold) biodegradation time. Recently sulfo-SMCC was found to play a major role in SAPs stiffness tuning. Sulfo-SMCC is a heterobifunctional cross-linker reacting with primary amines and sulfhydryl groups. It increased stiffness from 5 to 170 KPa (34 $\times$ ) and failure stress from 55 Pa to 3KPa (55 $\times$ ) in self-assembled (LKLK)<sub>4</sub> hydrogels previously functionalized with Cys residues.<sup>118</sup>

#### 4. PROCESSING OF SELF-ASSEMBLING PEPTIDES

Processing of peptide hydrogels can be confidently considered a mandatory step for the SAP technology to catch up with the

number of heterogeneous applications of other biomaterials in regenerative medicine. If processing is undertaken in aqueous solutions, always a preferred choice for tissue engineering applications, careful attention has to be paid in order to use the peptide hydrogels between the critical aggregation concentration and the maximum concentration allowed by its intrinsic solubility. However, in the case of more demanding processing requirements such as high viscosity and shear-thinning behavior, there is the need for highly concentrated solutions of SAPs in organic solvents, bringing potentially cytotoxic chemicals.<sup>129</sup> This shortcoming can be partially overcome by adopting multiple postprocessing steps to remove leftovers from the scaffold production. Examples of top-down techniques successfully used for processing of SAPs include: (i) microcontact printing of thiol-terminated peptides,<sup>62</sup> (ii) vapor deposition<sup>130</sup> and soft lithography<sup>131</sup> of short aromatic SAPs, (iii) scanning probe lithography of nanotubes made of PAs,<sup>132</sup> microfluidic systems for controlled self-assembly of SAPs,<sup>133</sup> and liquid injections of preheated hydrogels of self-aligned PAs.<sup>134</sup> However, most of them allow for the production of mainly 2D surfaces or 3D microscaled fragile scaffolds, suggesting the need for processing techniques better controlling the 3D nano- and micromorphology of SAP scaffolds to be used in regenerative medicine: this is the case electrospinning and 3D printing techniques described in the following section.

#### 4.1. Electrospinning of Self-Assembling Peptides

Self-assembly of peptides yields well-defined assembled molecular structures including  $\beta$ -sheets and  $\alpha$ -helices lacking a specific order at higher levels of assembly, *i.e.*, at the microscale. SAP scaffolds are usually hydrogels made of randomly assembled nanofibers, nanorods, nanoribbons, or nanotubes. This is in stark contrast with highly organized 3D cellular architectures of most tissues, where the wrong spatial orientation of cells and ECM components may dramatically compromise their biological functions and/or mechanical properties (*e.g.*, neural, muscle, and bone tissues). In contrast, electrospinning of peptides is a versatile technique commonly used with a number of high-molecular weight, natural (collagen I, cellulose, alginate, *etc.*),<sup>135</sup> and synthetic (poly lactic-co-glycolic acid, polycaprolactone, *etc.*) biomaterials,<sup>136,137</sup> allowing for the production of scaffolds comprising, among others, aligned<sup>135,136</sup> radially-<sup>138</sup> or circularly oriented<sup>136</sup> nano- and microfibers, and multilayered coaxial fibers also useful for drug delivery.<sup>36,139</sup> Intrinsically low-molecular-weight SAPs have been difficult to electrospin, as they do not provide sufficient widespread chain entanglement to warrant a stable spinning.

In some cases, this drawback forces researchers to shift from SAP-based approaches to composite electrospun scaffolds made of polymeric electrospun channels and SAP-fillers<sup>36</sup> or to electrospun blends of synthetic polymers, providing molecular entanglements and physical support, and SAPs in order to merge biofunctionalization and high biocompatibility with 3D spatial orientation.<sup>36,93,140,141</sup> Electrospinning of pure-SAPs was achieved with diphenylalanine peptides,<sup>142</sup> peptide amphiphiles,<sup>143</sup> and with a heterogeneous library of co-assembling and SAPs.<sup>129</sup> In the latter case electrospinning of nano- and microfibers was achieved for high concentrations of (LDLK)<sub>4</sub>, (RADA)<sub>4</sub>, (LKLK)<sub>4</sub>, (LDLK)<sub>4</sub>, and BMHP1-based peptides, at different chain lengths and with various functionalization. Dense solutions of SAPs provided sufficient chain entanglement, while organic solvents were necessary to increase solubility and

destabilize  $\beta$ -sheet formation before electrospinning, as it turned out to be detrimental to overall process.

Standard  $\beta$ -sheet formation is likely triggered by the laminar flow of the peptide solution and a strong electric field inside the injection needle of the electrospinning setup, bestowing sufficient fiber–water stability and functional motif exposure for biomimetic applications. The main issue with all of these approaches is that despite the seamless morphology of the electrospun SAP nets, their high porosity biomechanical properties are insufficient for providing other than just nanostructured coatings. This drawback was recently overcome by using genipin cross-linking before and after electrospinning of FAQ-(LDLK)<sub>3</sub>, a biomimetic SAP with neuroregenerative properties.<sup>37,119</sup> The authors managed to obtain flexible, self-standing, bioabsorbable, fibrous mats and microchannels from pure solutions of FAQ-(LDLK)<sub>3</sub> without affecting its standard  $\beta$ -structure and preserving the bioactivity of the FAQ functional motif<sup>119</sup> (Figure 9). SAP electrospinning may now potentially be fully exploited in diverse tissue engineering applications (*e.g.*, biomimetic bioabsorbable cardiac patches, nervous guidance channels, microvessel replacements, *etc.*) in the near future.

#### 4.2. 3D Printing of Self-Assembling Peptides

The 3D printing of cell tissue using various biocompatible polymers has been attempted but significant challenges remain.<sup>144</sup> In 2004, Sanjana and Fuller reported the design of a gel inkjet printer and used it to print neuron-adhesive specific patterns such as islands and characters “MIT” using polyethylene glycol (PEG) as the cell-repulsive material and a collagen/poly-lysine gel as the cell-adhesive material. They showed that dissociated rat hippocampal neurons and glia grown at low densities on such patterns retained arbitrary and strong pattern adherence for over 25 days.<sup>145</sup> This simple gel printer stimulated 3D scaffold/cell printing.

A significant advance in electrospinning is 3D scaffold/cell printing that is capable of providing very complex spatial arrangements of fibers and pores in different directions. 3D printed culture systems are now widely used in tissue cell fields.<sup>146–150</sup> It is used in biomedical research on designing organs for transplantation, prosthetics, medical implants, and 3D tissue models for various uses.<sup>151</sup> One of the main goals of tissue engineering research is the development *in vitro* of organs suited for subsequent implantation in patients, hence requiring 3D scaffolds that closely resemble the complex architectures of native tissues.

Researchers have become increasingly confident of its potential in providing patients with severe disease conditions with personalized scaffolds. Suitable hydrogels or bioinks with enhanced injectability, appropriate gelation kinetics in aqueous solutions, and at the same time biomimetic properties fostering cell viability and differentiation, were lacking. Raphael *et al.* reported the first 3D printing of a set of commercially available SAPs encapsulating mammary epithelial cells, demonstrating their viability and proliferation state *in vitro*.<sup>152</sup> By tuning various printing parameters Nolan *et al.* optimized their printing setup for a Fmoc-diphenylalanine SAP, so as to obtain multilayer printed structures, hypothesizing that organic solvent-triggered gels containing localized spherical domains of fibers feature better printability, as they flow more freely inside the injector without destroying the microstructure of their self-assembled network, and with less effect on the physical integrity of the final printed construct.<sup>147</sup>

**Table 2. Various Uses of SAPs Used in 3D Tissue Cell Cultures, Preclinical Tissue Repair, Tissue Regeneration, and Tissue Engineering**

self-assembling peptide	self-assembled secondary structure	nanostructure	ref
Neural Stem/Progenitor Cells 3D Cultures			
(RADA) <sub>4</sub> , (RADA) <sub>4</sub> functionalized with RGD, BMHP1, IKVAV	cross- $\beta$	tabular nanofiber	23,116,144,145
(LDLK) <sub>3</sub> functionalized with KLPGWSG, FAQRVPP, branched (LDLK) <sub>3</sub>	cross- $\beta$	tabular nanofiber	37,54,105
PA functionalized with IKVAV	$\beta$ -sheet	cylindrical nanofiber	183
Osteogenic Differentiation in 3D Cultures			
(RADA) <sub>4</sub>	cross- $\beta$	tabular nanofiber	156,157
3D Cultures of Epithelial Cells			
laminin-adsorbed (RADA) <sub>4</sub>	cross- $\beta$	tabular nanofiber	158
3D Cultures of Liver Cells			
(RADA) <sub>4</sub>	cross- $\beta$	tabular nanofiber	159
3D Cultures of Cardiac Progenitors			
RADA-II functionalized with mimicry of Notch1 ligand	cross- $\beta$	tabular nanofiber	101
Encapsulating Vehicle of Pancreatic Islets			
(RADA) <sub>4</sub>	cross- $\beta$	tabular nanofiber	160
Ischemic Heart Regeneration			
RADA-II, RADA-II tethered to IGF-1, PDGF-BB, RADA-II functionalized with mimicry of Notch1 ligand	cross- $\beta$	tabular nanofiber	100,101,161–164
(RADA) <sub>4</sub> tethered to S-SDF-1 (S4V)	cross- $\beta$	tabular nanofiber	165
(RADA) <sub>4</sub> loaded in porous elastomeric membranes	cross- $\beta$	tabular nanofiber	166
Cartilage Regeneration			
(KLDL) <sub>3</sub> , (KLDL) <sub>3</sub> imbued with TGF- $\beta$ 1, (KLDL) <sub>3</sub> functionalized with neuropeptide substance P, N-cadherin mimicry	cross- $\beta$	tabular nanofiber	99,167–171
PA functionalized with sulfate groups, binding sites for TGF- $\beta$ 1, Ser-linked $\beta$ -D-glucose and carboxylic acids	$\beta$ -sheet	cylindrical nanofiber	96,98,172
SAPs/synthetic polymers blends/coatings	cross- $\beta$	tabular nanofiber	150,173,174
Bone Regeneration			
(RADA) <sub>4</sub> , (RADA) <sub>4</sub> imbued with BMP-2	cross- $\beta$	tabular nanofiber	175,176
d-(RADA) <sub>4</sub> imbued with $\beta$ FGF	cross- $\beta$	tabular nanofiber	177
SPG-178-GEL	cross- $\beta$	tabular nanofiber	178
PA functionalized with RGDS, DGEA, phosphoserine residues, GAG-peptide mimicry and K-motif, alkaline phosphatase-peptide mimicry, loaded with HA nanoparticles	$\beta$ -sheet	cylindrical nanofiber	97,179–182
Spinal Cord Injury Regeneration			
PA functionalized with IKVAV	$\beta$ -sheet	cylindrical nanofiber	173,174
(RADA) <sub>4</sub> , (RADA) <sub>4</sub> functionalized with BMHP1, (RADA) <sub>4</sub> functionalized with BMHP1 and loaded into PCL/PLGA electrospun microchannels	cross- $\beta$	tabular nanofiber	36,185,186
(LDLK) <sub>3</sub> , (LDLK) <sub>3</sub> functionalized with FAQRVPP, multifunctionalized and mixed with (LDLK) <sub>3</sub> -branched SAP	cross- $\beta$	tabular nanofiber	37,54,187
(LDLD) <sub>3</sub> and (LKLK) <sub>3</sub> co-loaded into PCL/PLGA electrospun microchannels	cross- $\beta$	tabular nanofiber	111

Table 2. continued

self-assembling peptide	self-assembled secondary structure	nanostructure	ref
Spinal Cord Injury Regeneration			
$K_2(QL)_6K_2$	cross- $\beta$	tabular nanofiber	188–190
Brain Injury Regeneration			
$(RADA)_4$ , $(RADA)_4$ functionalized with epitope from BDNF	cross- $\beta$	tabular nanofiber	25,191–195
PA functionalized with epitope from Tenascin-C	$\beta$ -sheet	cylindrical nanofiber	196
Peripheral Nerve Transection Regeneration			
PA imbued with Sonic Hedgehog	$\beta$ -sheet	cylindrical nanofiber	197
PA and loaded into a blood vessel-channel, PA functionalized with RGDS and loaded in PLGA channels	$\beta$ -sheet	cylindrical nanofiber	198,199
$(RADA)_4$ , $(RADA)_4$ functionalized with BMHP1, RGD, IKVAV and loaded in PLLA/PLGA electrospun channels, $(RADA)_4$ functionalized with mimicry of NGF/BDNF and loaded in chitosan tubes	cross- $\beta$	tabular nanofiber	200–203

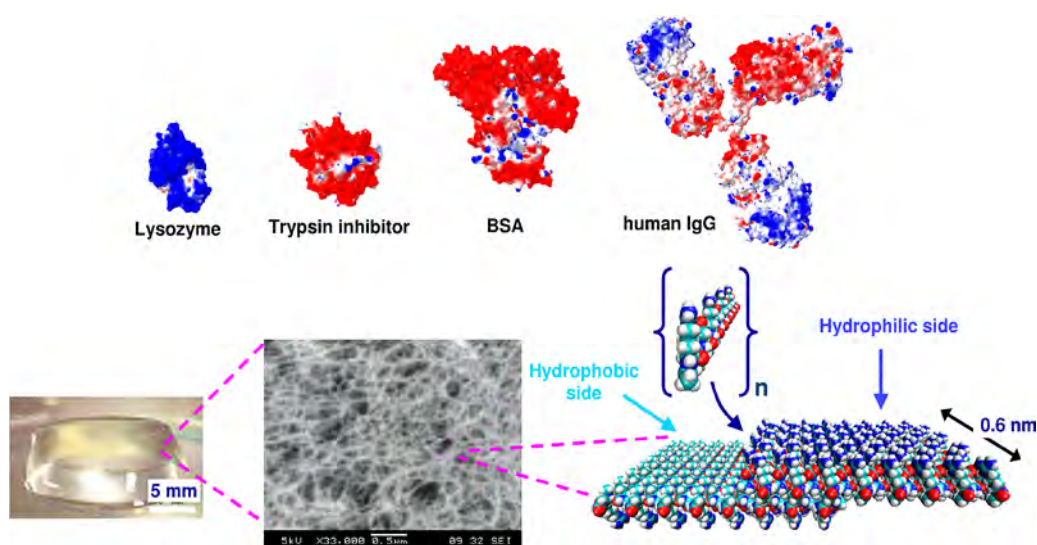


**Figure 10.** Molecular representations of lysozyme, trypsin inhibitor, BSA, and human IgG as well as of the Ac-N-(RADA)<sub>4</sub>-CONH<sub>2</sub> peptide monomer and of the peptide nanofiber. Color scheme for proteins and peptides: positively charged (blue), negatively charged (red), and hydrophobic (light blue). Protein models were based on known crystal structures. Image courtesy of Sotirios Koutsopolous. Reproduced with permission from ref 31. Copyright 2009 U.S. National Academy of Sciences.

Nonetheless, because of the intrinsically modest mechanical properties of SAPs, mixing polymeric biomaterials, and SAPs to achieve both weight-bearing and biomimetic properties is still the preferred strategy to date. To this purpose, other groups have 3D-printed ultrashort SAPs encapsulating muscle myoblast cells<sup>148</sup> or mixed functionalized PAs with thiolated-gelatin bioinks to provide biomimetics and, after dual cross-linking of the construct, achieved mechanical stability favoring the formation of tubular structures from encapsulated cholangiocytes, *i.e.*, bile ducts, *in vitro*.<sup>94</sup> Jung's lab 3D-printed poly(L-lactide-*co*-caprolactone) and RADA-based SAPs coupled with substance P and seeded with human dermal fibroblasts to treat skin defects: at four weeks after subcutaneous implantation in mice, they reported the beneficial effects (high deposition of collagens, blood vessel infiltration, and recruitment of mesenchymal stem cells) given by the biomimetic properties of the functionalized SAP mixed in the used bioink. Li *et al.* coated 3D-printed polycaprolactone scaffolds with FEFKFK

SAP to successfully stimulate the regeneration of cartilage and subchondral bone *in vivo* after three months in rabbits.<sup>149</sup>

## 5. APPLICATIONS OF SELF-ASSEMBLING PEPTIDE MATERIALS

Unlike many other nanobiomaterials using either nanoparticles for drug delivery purposes or nanostructured scaffolds after complex processes (electrospinning, vapor phase nucleation, etc.), SAPs feature the advantage of being synthetic but intrinsically prone to formation by either nanoparticles or nanostructured solid substrates depending on their sequence.<sup>66</sup> SAPs perfectly match the current need for biomimetic tunability required by most tissue engineering approaches,<sup>107,150,153</sup> but despite the very recent advances in mechanical tunability and 3D spatial organization, they have mainly been used as *in vitro* 3D systems as soft fillers or blended with stiffer synthetic polymers (Table 2).

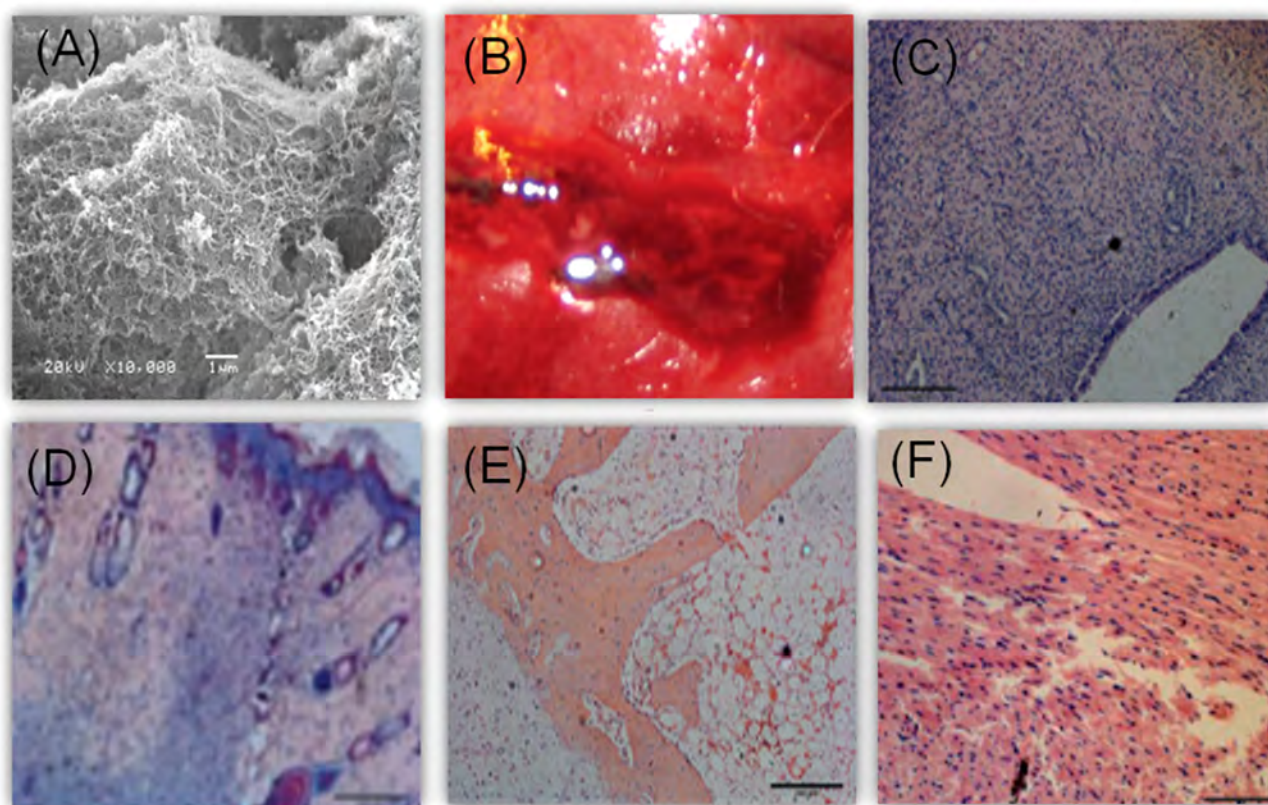


**Figure 11.** SAP used in various areas. (A) Used in 3D tissue cell culture. (B) Rapid hemostasis to stop bleeding. (C) Accelerated rat skin wound healing. (D) Accelerated rat uterus wound healing. (E) Accelerated rabbit articular cartilage injury repair. (F) Promotion of rat myocardial infarction repair.

### 5.1. Self-Assembling Peptide Materials in Controlled and Sustained Molecular Releases

Robert Langer pioneered the controlled and sustained releases of various molecules, peptides, proteins, DNA, and RNA for therapeutic and common uses.<sup>204</sup> His lab has developed biocompatible polymers for all kinds of uses including tissue repair and tissue engineering.<sup>194</sup> Inspired by Langer, researchers are seeking to utilize SAP scaffolds to achieve long-term, sustained molecular release. Because SAPs form nanofiber scaffolds with nanopores in a dynamic process over time, researchers seek to utilize this SAP hydrogels to deliver a range of substances, from a few nm to  $\sim 100$  nm, such as antibodies, for controlled delivery in molecular medicine.<sup>31,205–207</sup>

The SAPs EAK16-II, RAD16-II, and RAD16-I have been used as a model to slow the release of hydrophobic molecules from weeks to months, showing that these types of SAP scaffolds can encapsulate and deliver hydrophobic therapeutics. Various dye molecules including phenol red, bromophenol blue, 8-hydroxypyrene-1,3,6-trisulfonic acid trisodium salt, 1,3,6,8-pyrenetetrasulfonic acid tetra-sodium salt, and Coomassie Brilliant Blue G-250 through RADA16 hydrogels, provide an alternate route of controlled release of small molecules.<sup>205</sup> Furthermore, nanofiber-encapsulated camptothecin and ellipticine have been confirmed to inhibit tumor growth.

SAP scaffolds have also been used for the sustained release of proteins including lysozyme, trypsin inhibitor, BSA, MMP-13, and monoclonal antibody IgG (Figure 10),<sup>31</sup> and active cytokines bFGF, TGF, VEGF, and BDNF.<sup>206</sup> Furthermore, they can be used for sustained release from a few days to over 100 days (>3 months) when the experiments were termi-

nated.<sup>207</sup> It is likely to be sustained-release much longer because the content had not decreased significantly when the experiment results were collected.<sup>207</sup>

### 5.2. Self-Assembling Peptide Materials in Tissue Repair

Among the best advantages of SAPs is the ability to fine-tune designs at a single amino acid level and the ability to produce the designs with very high purity. SAP designs can incorporate specific features for individual tissues of interest, or a combination of features to accommodate specific needs, depending on their sequence.<sup>66</sup> Furthermore, SAP materials can be designed to perfectly match any need for biomimetic tunability required for most tissue repair and tissue engineering.<sup>107,150,153</sup> They can also be blended with various stiffer synthetic biocompatible polymers. With recent advances in mechanical tunability and 3D spatial organization, designer SAPs have been used as *in vitro* 3D tissue culture systems, as soft fillers for tissue repair, for rapid hemostasis, accelerated skin and uterus wound healing, articular cartilage injury repair, as well as myocardial infarction repair (Figure 11).

**5.2.1. 3D Niches for Stem Cell Culturing and Differentiation.** Given the ease of biomimetic functionalization, the well-self-assembled nanostructured morphology, the good biomechanical tunability, the high ratio of water-to-medium (95–99%), the satisfactory permeability and, most importantly, the excellent transparency, SAPs are a highly preferred choice for the design of synthetic microenvironments coaxing stem cell differentiation *in vitro*. The type and density of functional motifs can dramatically influence stem cell fate, but hydrogel stiffness also plays an important role as demonstrated by Engler et al.<sup>113</sup> RGD and BMHP functional motifs have been successfully linked

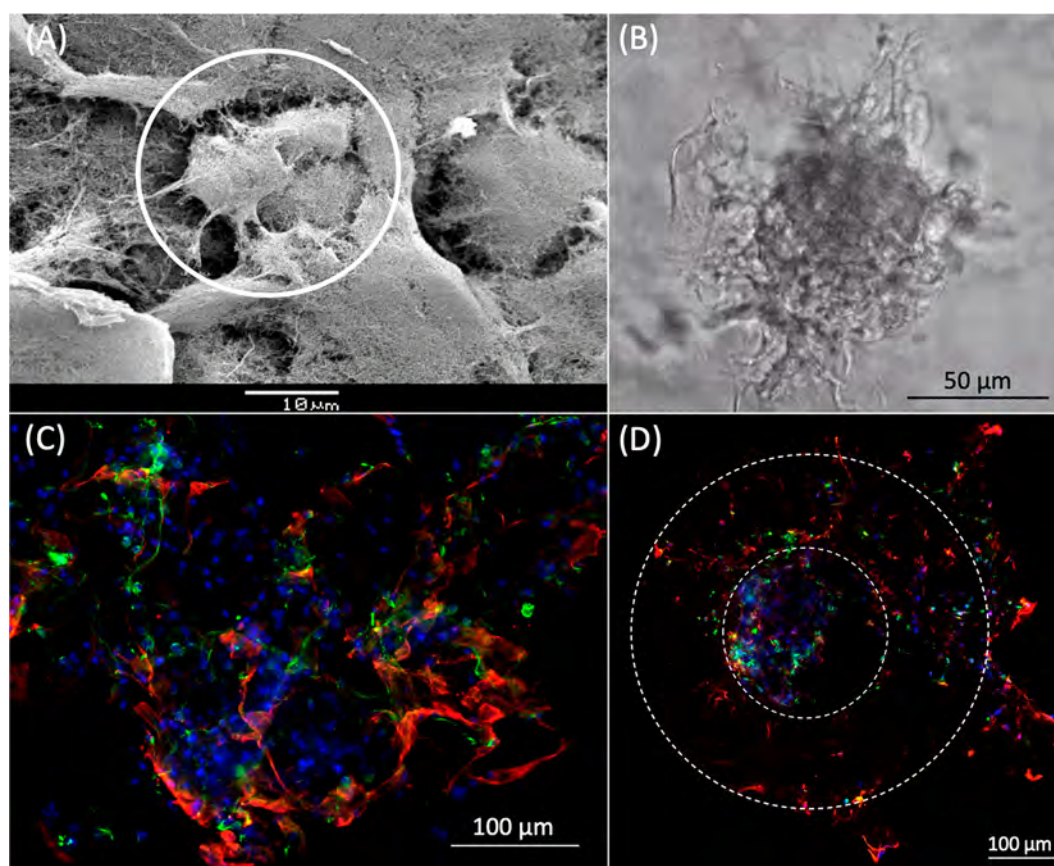


**Figure 12.** Self-assembling peptides as 3D tissue cell culture systems. (A) SEM image of murine neural stem cells (white circle) embedded in BMHP1-(RADA)<sub>4</sub> nanofiber scaffold similar in the body. Reproduced with permission from ref 30. Copyright 2009 PLOS. (B) Optical image of a neurosphere comprising several murine neural stem cells. At 2 DIV, cells extend protrusion and migrate from the inner core of the sphere to the outer transparent and functionalized SAP-made scaffold. (C) 3D construct of human NSCs cultured for six weeks *in vitro* in HYDROSAP multifunctionalized SAP-hydrogel.<sup>50</sup> An entangled network of neurons (βIII-TUB in green) and astrocytes (GFAP in red) can be appreciated. (D) Cross-section of hNSCs injected inside a functionalized (and cross-linked) SAP-made electrospun microchannel (dashed lines outline channel walls) and cultured for two weeks *in vitro*. Microchannels have been developed to guide nervous regeneration in spinal cord injuries. Neurons are marked in green (βIII-TUB) and astrocytes in red (GFAP). Cells initially seeded inside the inner lumen migrated infiltrating the channels walls. Images (C) and (D) are courtesy of Amanda Marchini.

to RADA16-I, also called (RADA)<sub>4</sub>, to trigger proliferation, differentiation, and neurite outgrowth of NSCs in 3D systems.<sup>23,116</sup> (Figure 12A,B) Cunha *et al.* reported that softer SAP-hydrogels favored NSC proliferation and neuronal differentiation similarly for each chosen functional motif. Sun *et al.* showed how double functionalization of (RADA)<sub>4</sub> with RGD and IKVAV (two oppositely charged SAPs at neutral pH) can actually improve viability and differentiation of NSCs over single functionalization.<sup>154</sup> Notably, (LDLK)<sub>3</sub> functionalized with phage display-derived functional motifs KLPGWSG and FAQRVPP showed neuronal and oligodendroglial differentiation superior to the standard positive controls (Cultrex BME).<sup>37,105</sup>

Recently a remarkable advance was reported by Marchini *et al.*, where a refined composition of multiple-functionalized (LDLK)<sub>3</sub>-based SAPs, mixed with branched (LDLK)<sub>3</sub> to provide optimized mechanical stiffness, and enables the formation of a dense 3D network of differentiated and electrically active mature neurons, astrocytes and oligodendrocytes in long-term cultures (Figure 12C). They managed to obtain GABAergic, glutamatergic, and cholinergic neurons as well as cells expressing basic myelin proteins in serum-free cell cultures from human GMP-grade NSCs, with potential

translation into nervous patches for spinal cord injury regeneration and/or *in vitro* model of nervous tissue.<sup>54</sup> PAs functionalized with IKVAV laminin-derived epitope also showed neurogenic properties in 3D cultures of progenitor cells while decreasing percentages of astroglial cells.<sup>183,184</sup>

Herland's lab showed that 3D cultures of stem cell-derived neurons in RADA16-I, as opposed to conventional 2D cultures, can mimic pathological changes typical of Alzheimer's disease caused by Aβ oligomers, such as redistribution of pPAK and drebrin, therefore suggesting that 3D cultures are very important as a more refined model in studies of mechanisms and potential treatments of Alzheimer's disease.<sup>155</sup>

3D culture using RADA16-I scaffolds for mouse neural stem cells differentiation toward both neuronal and glial phenotypes in *in vitro* serum-free condition was carried out by Zou *et al.*<sup>156</sup> Enhanced osteogenic differentiation was also reported by Chen *et al.* using 3D cultures of MSCs and repeated heat shocks in RADA16-I scaffold.<sup>157</sup> Laminin-adsorbed RADA16-I was used by Miroshnikova *et al.* to obtain acinar morphogenesis from mammary epithelial cells and, in the case of stiffer gels, invasive epithelial tumor-like phenotype and tumor-promoting genes upregulation, useful for a better understanding of epithelial morphogenesis.<sup>158</sup> Aiming to obtain a clinical-grade bioartificial

liver, RADA16-I was used to 3D culture primary rat liver cells in a clinically relevant bioreactor, a finding found desirably stable (up to one month) liver gene expression as well as essential biochemical liver functions including detoxification and biotransformation.<sup>159</sup>

Boopathy *et al.* synthesized RADA-II functionalized with a biomimicry of the Notch1 ligand Jagged1 to stimulate proliferation and growth factor production of cardiac progenitor cells *in vitro*.<sup>101</sup> Song's lab evaluated how SAPs can also be used as efficient encapsulating vehicles for pancreatic islets from rats in order to improve their viability and insulin secretion *in vitro*, a useful step to improve the current state-of-the-art of pancreatic islets clinical transplantation usually limited by lack of donors and short-term reliability of *in vitro* pancreatic islets cultures.<sup>159</sup> The numerous examples we report here are not exhaustive, but are intended to provide the flavor of the potential impact of SAPs in 3D culturing of almost all types of cells.

**5.2.2. Ischemic Heart Disease (IHD).** One of the most common applications is for hydrogel-based biomaterials in infarcted myocardia that comprises repeated injections in and around the injured area in order to alter the physiological remodeling of heart tissue to minimize scar tissue and subsequent dysfunction after infarct.<sup>208</sup> Historically, one of the first applications of SAPs in ischemic heart disease (IHD) came from a study by Davis *et al.*<sup>161</sup> They tethered IGF-1 (insulin-like growth factor 1), a growth factor for cardiomyocytes, to RADA-II (AcN-(RARADADA)<sub>2</sub>-C-NH<sub>2</sub>) via a biotin–streptavidin sandwich and achieved sustained release of IGF-1 *in vivo* for 28 days. By adding cardiomyocytes to the SAP injections, the myocyte cross-sectional area was increased by 25% and systolic function was improved in rats. They showed increased recruitment of stem cells and improved cardiac function in animals receiving the decorated SAP.<sup>165</sup> Others showed that injections of RADA-II SAP solution with PDGF-BB allowed for 14-day sustained delivery in IHD rats, decreasing cardiomyocyte death and infarct size.<sup>162</sup>

Hsieh's lab brought the "SAP-injection" approach to medium-size animals. They injected RADA-II alone or in combination with bone marrow mononuclear cells into the myocardia of IHD pigs, obtaining a significant improvement in the diastolic function (for scaffolds alone and scaffolds with cells) and in the systolic function (for scaffolds injected with cells) of the injured heart.<sup>163</sup> Boopathy *et al.* tested the therapeutic potential of RADA-II functionalized with a mimic of Notch ligand Jagged-1, interspaced by a 7-glycine linker, in order to trigger the activation of the endogenous healing response following infarct: first, they showed how *in vitro* 3D cultures Notch1 expression in cardiac progenitor cells was strongly correlated to the presence of Jagged-1 mimicry and to SAP stiffness, they then demonstrated an improvement in cardiac function back to sham-operated levels, with a significant decrease in fibrosis and increase in blood vessel area.<sup>100,101</sup>

Recently, Kim *et al.* targeted the regenerative potential of adipose stem cells predifferentiated *in vitro* into 3D spheroids of vascular cells, after cop-transplantation with RADA-II in IHD rats. At four weeks *in vivo* they showed the cell-seeded SAP improved by 3-fold the survival rate of transplanted cells, reduced the overall infarct size and increased both localized angiogenesis and myocardium ejection fraction and arterial elastance.<sup>164</sup> Castells-Sala *et al.* reported the use of RADA16-I with motifs of SKPPGTSS, FHRIKA, or PRGDSGYRGDS to control human adipose stem cell behavior. They found the scaffolds promoted higher cell proliferation, migration, and the

secretion of angiogenic growth factors. These findings have potential for regenerative medicine and stem cell therapies.<sup>166</sup>

**5.2.3. Cartilage.** Hydrogel-based tissue engineering approaches for cartilage regeneration have made considerable advances in recent years.<sup>167,168,209</sup> Cartilage is an avascular and non-neural tissue comprising collagens, proteoglycans, and chondrocytes differentiated from chondroblasts, with limited self-repairing capability and lubricating behavior. Cartilage defects are a cause of major disabilities such as osteoarthritis (OA). Therapeutic approaches include implants of stem cells, autologous chondrocytes or acellular scaffolds from natural sources (*e.g.*, collagen, hyaluronic acid) or synthetic origin (*e.g.*, PLGA, PEG, carbon fibers).<sup>210,211</sup> Hydrogels are currently preferred because of their lubricating behavior and swelling ability. Among them, SAPs feature the advantage of being biomimetic, nanostructured similarly to ECM, mechanically tunable, and synthetic. The first major advance in the field was obtained by Cassidy *et al.* with (KLDL)<sub>3</sub> peptide. They developed an *in vitro* protocol for four-week culturing phenotypically stable chondrocytes and production of a mechanically stiff tissue rich in type 2 collagen and proteoglycans *in vitro*.<sup>167</sup> They also managed to obtain cartilage-like deposition from adult bone marrow stromal cells cultured in (KLDL)<sub>3</sub> superior to that obtained with standard chondrocytes.<sup>168</sup> TGF- $\beta$ 1 is an important growth factor regulating cell proliferation and differentiation in chondrogenesis. Peptide amphiphiles were functionalized with binding sites for TGF- $\beta$ 1 to induce its slow release once loaded into the hydrogel, favoring chondrogenic differentiation from human mesenchymal stem cells and cartilage regeneration in rabbits.<sup>104</sup>

(KLDL)<sub>3</sub> previously imbued with TGF- $\beta$ 1 and other growth factors and seeded with allogenic bone marrow stromal cells was tested in osteochondral defects *in vivo*, showing that rabbits receiving SAPs alone presented the best cartilage repair after 12 weeks.<sup>169</sup> *In vitro* cultures of prechondrogenic cells seeded in PAs previously functionalized with sulfate groups, mimicking sulfate molecules usually found in ECM of cartilage, showed formation of cartilage-like nodules and deposition of cartilage ECM components, confirmed by gene expression analyses testifying chondrogenic differentiation *in vitro*.<sup>172</sup> (LDLK)<sub>3</sub> was also functionalized with neuropeptide substance P, known to play a role in cell proliferation, regulation of wound healing but also functioning as a chemotactic factor through mobilization of MSCs into circulation and, most importantly, playing an anti-inflammatory role in rheumatoid arthritis.<sup>170</sup> Authors reported that decorated (LDLK)<sub>3</sub> facilitated the long-term release of SP in rats with induced osteoarthritis, providing a favorable environment for cartilage regeneration at the defect site. SAP-SP prevented apoptosis, favored extracellular matrix deposition and alleviated the inflammation in osteoarthritis.<sup>161</sup>

Guler's lab reported the co-assembly of PAs functionalized with a Ser-linked  $\beta$ -D-glucose and carboxylic acids, in mimicry of hyaluronic acid. After self-assembling, PA nanofibers displayed multiple glucose residues in close proximity, inducing chondrogenic differentiation of mesenchymal stem cells (MSCs) similar to hyaluronic acid, and favored the deposition of hyaline-like cartilage in rabbits with osteochondral defects.<sup>96</sup> (LDLK)<sub>3</sub> was also functionalized with N-cadherin (heavily involved in cell–cell interactions and organ development) mimetic peptide and seeded with human hMSCs. Their construct led to type 2 collagen deposition and chondrogenic differentiation through suppression of canonical Wnt/ $\beta$ -catenin signaling of hMSCs.<sup>99</sup> Recently, (LDLK)<sub>3</sub> was also used as a

standard for cartilage cell cultures in order to demonstrate how human osteoarthritic chondrocytes *in vivo* can actually outperform human osteoarthritic chondrocytes *in vitro* in terms of survival and deposition vs degradation of type 2 collagen, with potential implications in future clinical therapies.<sup>211</sup> Despite many publications, SAP applications in cartilage repair are still limited by their modest mechanical properties. This is the reason why a good number of studies employing composite SAP-polymeric scaffolds flourished in the past decade.<sup>150,173,174</sup> However, covalent cross-linking of SAPs<sup>118,119</sup> may be considered in the near future to fill this gap.

**5.2.4. Bone.** Bone is a dynamic and vascularized tissue usually characterized by high stiffness and moderate self-healing capability. In the case of large bone defects, the gold standard of clinical practice is bone autograft, when available, or allo- and xenografts. In the first case, major limitations are donor site morbidity, pain, and paresthesia,<sup>212</sup> while, for the second option, concerns about pathogen transfer, immunologic reactions, and reduced bioactivity still limit their usage.<sup>213</sup> A good number of synthetic ceramic or polymeric scaffolds have been tested for bone repair,<sup>214</sup> but biomimetic microenvironments promoting bone ingrowth and implant integration were difficult to obtain.<sup>215</sup> Therefore, scaffolds coaxing osteogenesis, osteoconduction, featuring physiological mechanical support, high porosity favoring nutrient exchange, and displaying bioactive molecules enticing host cells ingrowth and/or transplanted mesenchymal stem cells (MSC) engraftment are still greatly needed.<sup>153</sup>

Most of these requirements can be met by SAPs, and that is the reason why a number of works flourished with RADA-like and peptide amphiphile hydrogels. RADA16-I was shown to foster mature bone formation in calvaria bone defect in mice with satisfactory tissue strength<sup>175</sup> and increased cortical bone regeneration in rabbits when previously loaded with recombinant bone morphogenic protein BMP-2.<sup>176</sup> Also, D-form amino acids have been used in tissue engineering to extend SAP bioabsorption time because L-proteases do not degrade D-peptide bonds. d-RADA16 hydrogels loaded with basic-fibroblast growth factor ( $\beta$ FGF) promoted bone repair in femoral condyle defects in rats.<sup>177</sup> Another RADA-like SAP, dubbed SPG-178-Gel, was successfully used to achieve new bone formation in rat calvarial defects and osteogenic induction of dental pulp stem cells when exposed to an osteogenic induction medium in both two- and three-dimensional cell culture setups.<sup>178</sup>

Traditionally, functional peptide motifs for bone regeneration have been derived from fibronectin (RGDS), collagen I (DGEA), and glycosaminoglycans, all major components of bone extracellular matrix. Peptide amphiphile (PA) were functionalized with RGDS and phosphoserine residues to respectively improve cell attachment and nucleation of hydroxyapatite (HA), the major inorganic mineral in bone ECM, resulting in increased amount of ossified tissue within the callus of femoral defects (5 mm) in rats.<sup>179</sup> RGDS-peptide amphiphile, when co-assembled with DGEA-peptide amphiphile and loaded with HA nanoparticles (also added to improve mechanical stability) in a biphasic gel, was demonstrated to upregulate the expression of genes strictly correlated with osteogenic differentiation of human mesenchymal stem cell (hMSC) cultures, also promoting bone healing response in femoral defect rat models.<sup>97,180</sup> Osteo-inductive properties were also demonstrated for peptide amphiphile functionalized with both GAG-biomimetic peptide and positively charged motif K,

favoring hMSC osteogenic differentiation *in vitro* and bone regeneration *in vivo*.<sup>181</sup> Peptide amphiphiles were also extended with a functional motif mimicking the active site of alkaline phosphatase to replicate its catalytic and matrix regulatory function in bone morphogenesis, enabling osteogenesis of mesenchymal and osteoblast-like cell lines.<sup>182</sup> Lastly, given the fact that so far functionalized SAP scaffolds usually may not have sufficient mechanical strength for weight bearing replacements they were used as coatings of titanium-based implants to facilitate implant osteointegration and formation of bone-like minerals,<sup>89</sup> or as pore fillers of metallic foams carrying MC3T3-E1 cells to achieve mineralization, vascularization, and bone formation in rat femur defects.<sup>216</sup>

### 5.3. Self-Assembling Peptide Materials in Nervous Regeneration

Spontaneous regeneration in nervous tissues varies consistently from central nervous system (CNS) to peripheral nervous system (PNS). In nerve injuries of limited magnitude (<2 cm) clinical practice includes allogenic implants from the patient's own donor sites or implantation of channels simply canalizing the spontaneous ingrowth of nervous fibers. In the case of larger PNS injuries, and most lesions at the CNS, a complex cascade of harmful events follow the initial injury, ending with its worsening and gliotic scar formation, hampering the development of any reliable clinical therapy to date. Nervous cells are highly sensitive to the bioactivity and the mechanical properties of the surrounding microenvironments. These are both facets that can be efficiently addressed by SAPs as nervous soft stiffness (100–1000 Pa)<sup>113,114</sup> easily falls within the range of SAP hydrogels and SAP biofunctionalization with laminin (one of the major components of basement membrane) moieties has already been reliably achieved by various groups.<sup>23,94,184</sup> On the other hand, flexibility/compliance in peripheral nerves and 3D spatial cytoarchitecture in both the CNS and the PNS are two requirements for nervous tissue regeneration that were only recently resolved through SAPs.<sup>118,119</sup> The new solutions have yet to be exploited.

**5.3.1. Spinal Cord Injury Repair.** Spinal cord injuries (SCIs) can be both traumatic and degenerative, but most importantly, in the acute phase (up to 1 year in humans) they differ quite a lot from chronic injuries. After the initial insult, the lesion is involved in a complex constellation of reactions comprising inflammation, necrosis, and axotomy. Over time, there is an enlarging of the initial lesion through apoptosis, demyelination, chronic inflammatory response, all leading to the formation of a gliotic scar often surrounding an aqueous cyst. In a few words, in chronic lesions the tissue function and cytoarchitecture are usually more compromised. On the other hand, in acute SCIs, and particularly in contusive lesions, there is limited room for solid scaffolds implantation unless surgical excisions are practiced, putting at risk the physiological development of the tissue reaction.

The first notable work in this area was published by Kessler's lab: they injected IKVAV-functionalized peptide amphiphiles in acute SCIs, showing that SAP treatment reduced astrogliosis, reduced apoptosis, and increased the recruitment of oligodendrocytes to the site of injury. SAP scaffolds promoted regeneration of both descending motor fibers and ascending sensory fibers through the lesion site and caused significant behavioral improvement (Figure 13).<sup>183</sup> Later, they showed that IKVAV-PAs efficiently fostered serotonergic fiber presence that is crucial for locomotor recovery caudally to both contusive and



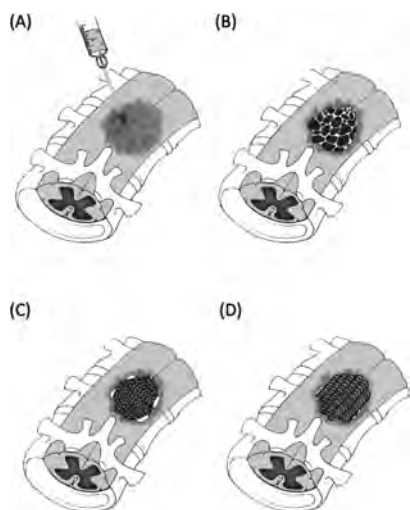


**Figure 13.** Schematic illustrations of different type of SAP hydrogel implants for spinal cord injuries. (A) aqueous solutions of SAPs were microinjected multiple times into acute SCI, triggering their assembly *in vivo* and filling the microcavities of acute contusive injuries. (B) preassembled and crumpled SAP scaffolds were subsequently positioned into previously debrided site on SCI injuries. (C) Preformed SAPs scaffold densely seeded with stem/progenitor cells, or with *in vitro* pre-differentiated stem cell progenies, were subsequently positioned into subacute surgical SCI. (D) composite scaffolds made of SAP hydrogels previously loaded into electrospun microchannels were positioned one by one along the spinal cord axis and into previously debrided gliotic scar/aqueous cysts found in chronic SCI. In initial experiments microchannels were made of polymeric materials, but recently they were produced entirely from cross-linked SAPs. In all cases, SAP can be functionalized with one or multiple functional motifs.

compressive chronic spinal cord lesions and improved functional recovery in both mice and rats.<sup>184</sup>

One of us (Gelain) with colleagues has made a number of advances in the field of SCI regeneration using SAPs. (RADA)<sub>4</sub> functionalized with BMHP1 functional motif in 3D NSC cultures<sup>23</sup> was used it as a filler of nanostructured microchannels made of electrospun PCL/PLGA to regenerate chronic contusive SCI in rats. When loaded with a mix of pro-regenerative cytokines significant nervous tissue regeneration and functional recovery was achieved by the end of the six-month experimental time frame. In acute SCI a similar SAP, characterized by a longer Gly-spacer designed to improve the efficacy of the BMHP1 functional motif, was injected into acutely injured SCIs sites in rats. Compared to the control, decreased inflammatory response, increased amounts of nervous fibers and increased expression of genes related to trophic factors synthesis and matrix remodeling were detected.<sup>186</sup>

The neuroregenerative potential of two different SAPs, (LDLK)<sub>3</sub>, and a BMHP1-derived SAP, were tested at different concentrations, correlating rheological properties of the injected scaffolds vs *in vivo* diffusion, hemostat, and neuroprotective properties.<sup>187</sup> Interestingly, main outcomes were that in acute SCI, only diluted SAPs (lowest  $G'$ ) showed appropriate diffusion within the injured tissue without perturbing the pre-existing neural circuitry, and both SAPs could attenuate hematoma and show neuroprotective effect testified by an increased number of regrown axons.

(LDLK)<sub>3</sub> functionalized with FAQRVPP phage display-derived functional motif also showed enhanced functional recovery and neural regeneration, supported also by decreased

lesion area and cyst cavities in acute SCI.<sup>37</sup> Later the same functional motif was applied to the co-assembling peptide (LDLD)<sub>3</sub>, co-loaded with its counterpart (LKLK)<sub>3</sub> into electrospun polymeric microchannels placed in complete transections at the spinal cord of rats. Again, they showed the functionalized SAP increased nervous regeneration within the channels, decreased cyst area, and fostered the presence of newly formed blood vessels infiltrating the channels.<sup>111</sup>

Recently, the same lab published a seminal work focused on both high-density 3D cell cultures and SCI regeneration. A construct made of a multifunctionalized (LDLK)<sub>3</sub>-based SAP previously mixed with a branched (LDLK)<sub>3</sub> sequence was used to provide optimized mechanical strength and densely seeded with GMP-grade hNSCs in long-term cultures. Although the results will never reach the complexity of an organoid *in vitro* (see 3D culture section for more details), electrically active neuronal networks were obtained. The therapeutic efficacy of the joint usage of these two technologies in surgical acute SCI was tested by implanting the construct at different times of maturation *in vitro* (1 day and 6 weeks).<sup>54</sup> Implants showed decreased inflammatory reaction and gliotic scar formation, but scaffolds with pre-differentiated hNSCs showed the highest hNSC engraftment and maturation, neuroregeneration and best functional recovery, therefore seemingly to better exploit the potential of stem cell therapy in tissue regeneration and repair of spinal cord injury.

Fehlings' lab injected K<sub>2</sub>(QL)<sub>6</sub>K<sub>2</sub>SAP immediately after cervical SCI in order to create a protective microenvironment favorable to subsequent (2 weeks later) neural progenitor cell (NPC) transplantation: results showed increased differentiation of NPCs toward neural and oligodendroglial phenotypes, decreased cyst volume and improved functional recovery.<sup>188</sup> The same group also tested the effect of a conjoint injection of SAP and NPC in the same SCI animal model at 14 days post-cervical SCI, finding decreased inflammation and improved behavioral recovery,<sup>189</sup> and the usage of SAP-only solution at 1 d post-SCI. They detail a decreased post-traumatic apoptosis, neuroinflammation, scarring, and improved behavioral and electrophysiological scores.<sup>190</sup>

**5.3.2. Stroke.** Brain tissue is subjected to minimal deformations and, as already mentioned above, is mainly a soft tissue. However, it has an extremely complex cytoarchitecture, namely, neural circuitry, is still largely unknown, hence unlike for other nervous tissue, most of the approaches do not seriously consider the spatial organization, or the regenerating tissues. The first research on the regeneration of acute brain injury using SAPs was reported by Ellis-Behnke et al.<sup>30</sup> They injected (RADA)<sub>4</sub> into freshly cut optical tracts in hamsters, reestablishing nervous projections and restoring part of impaired vision in treated animals. Recently various functionalized SAPs have been developed to enhance adhesion, proliferation, and differentiation of NSCs from the human and murine brains in both 2D and 3D fashion *in vitro*: thus, in principle, suggesting some regenerative potential for CNS injuries as well.<sup>23,37,38,54,105,116</sup>

The surgical brain injury was later filled twice with (RADA)<sub>4</sub> to stop bleeding and to provide a neuroregenerative substrate for cortex tissue ingrowth. Wu's lab also reported that SAP-treatment decreased inflammatory response and astrogliosis and reduced tissue loss after injury.<sup>191</sup> The same research group later in a rat model of acute cerebral hemorrhage showed that, after hematoma aspiration, local delivery of (RADA)<sub>4</sub> actually integrated well within the irregular cavities, replacing the

hematoma in the deep brain, reducing nervous cavity and promoting functional recovery.<sup>192</sup> (RADA)<sub>4</sub> was also reported as an efficient carrier for the delivery and grafting of human induced pluripotent stem cells (iPSCs) in the brain.<sup>193</sup> (RADA)<sub>4</sub> was functionalized with RGIDKRHWNSQ motif that is derived from brain derived neurotrophic factor (BDNF) and used as a cell carrier for the cotransplantation of human umbilical cord mesenchymal stem cells (MSC) and activated astrocytes to heal traumatic brain injuries in rats. The functionalized SAP favored MSC differentiation and engraftment *in vivo*, achieving regeneration of moderate-size cavities by stimulating axon, dendrite outgrowth, and synapse formation.<sup>194</sup>

Kuhn's lab reported a novel approach: looking for the recruitment and redirection of resident endogenous neuroblasts in the adult brain, they functionalized PAs with an epitope from Tenascin-C, known for its migratory and proliferative effects on neural precursor, and injected it into the rostral migratory stream in rodent adult brains to successfully lead an artificial migration of resident neural progenitor cells to the cortex and, in principle, to specific injured sites into the brain.<sup>196</sup> A recent multidisciplinary approach described by Nisbet *et al.* made use of an SAP scaffold functionalized with a Laminin-derived motif, loaded with BDNF, and seeded with embryonic stem cell-derived neural progenitors injected in stroke injuries: the combined therapy caused improved nervous differentiation and engraftment of transplanted cells and increased blood vessel infiltration into the implants, both favoring the protection of the surrounding ischemic areas.<sup>217</sup> Others also reported using (RADA)<sub>4</sub> as a carrier for epileptic brain-derived hNSCs and for human adipose-derived stem cells for the treatment of traumatic brain injuries. In both cases, they reported decreased neuro-inflammation, injury size, and reactive gliosis, suggesting the potential of combined therapies with SAPs for the treatment of traumatic lesions in the brain.<sup>195</sup>

**5.3.3. Peripheral Nerve Transections (PNT).** The first attempts to explicitly tackle peripheral nervous regeneration with SAPs were reported by Zou *et al.* using IKVAV-functionalized PAs to successfully culture dorsal root ganglion sensory neurons of rats *in vitro*,<sup>218</sup> and by Angeloni *et al.*, describing an effective *in vivo* release of Sonic Hedgehog from peptide amphiphiles injected into crushed cavernous nerves in rats.<sup>197</sup> Coping with the problem of producing SAP-based flexible channels mimicking nerve mechanical properties, Wu's lab proposed a hybrid solution comprising a channel made of a blood vessel filled with peptide amphiphiles to achieve axonal regeneration and remyelination throughout a 1 cm gap in sciatic nerve transections.<sup>198</sup> Others also tested the neurodegenerative potential of PLGA guidance channels filled with mechanically aligned nanofibers of RGDS-functionalized PAs in 12 mm long sciatic nerve defects. The encouraging results showed both behavioral recovery and nervous fibers regeneration close to nerve autografts.<sup>199</sup> Schwann cells (myelinating peripheral neurons) were successfully cultured *in vitro* on PLGA electrospun nanofibers decorated with RADA-BMHP1 peptides, demonstrating the positive effect of SAP decoration.<sup>14f</sup> They later aligned these same nanofibers into a single construct, which was implanted in transected rat sciatic nerves. The animals demonstrated improved neuro regeneration and sensorimotor function recovery in SAP decorated electrospun nanofibers.<sup>200</sup>

Wu *et al.* functionalized (RADA)<sub>4</sub> with RGD and IKVAV functional motifs. After mixing the two functionalized SAPs together, they loaded the hydrogel into electrospun PLLA microchannels sutured to two stumps of 5 mm gaps on sciatic

nerves. After 12 weeks they detected higher nervous ingrowth (compared to saline and to nonfunctionalized (RADA)<sub>4</sub>) crossing the lesions and better myelination.<sup>201</sup> Peptide amphiphile functionalized with a phage display-derived binding sequence for NGF were shown to have high affinity for NGF *in vitro* and to promote primary sensory neuron outgrowth *in vitro*.<sup>109</sup> In another work, (RADA)<sub>4</sub> was functionalized with two sequences mimicking NGF and BDNF (brain derived neurotrophic factor). Again, this SAP mix, after being demonstrated to foster PC12 cells outgrowth *in vitro*, was injected into chitosan tubes sutured to 1 cm long sciatic nerve defects, showing accelerated nervous regeneration and improved functional recovery.<sup>202</sup> Nonetheless, the same group in a subsequent paper showed similar improvements with (RADA)<sub>4</sub> functionalized with the BDNF-mimicking sequence alone.<sup>203</sup> The take-home message from peripheral nerve transection (PNT) regeneration may be that the promising functionalization is now available for SAPs. Although less optimal biomechanics have limitations for their uses, with the advent of cross-linked SAPs,<sup>118,119</sup> the blended materials will improve significantly. Other uses have been launched (Figure 12).

#### 5.4. Anticipated and Unanticipated Uses of Self-Assembling Peptide Materials

Although many SAPs form nanofibers or scaffold hydrogels, other SAPs form different nanostructures, thus with different applications. For example, Gazit's lab has discovered that phenylalanine–phenylalanine (FF) with a single peptide bond can form remarkably stable nanotubes and other nanostructures under various conditions.<sup>219</sup> They found that nanostructures from the simplest dipeptide FF can: (a) encase silver ions to form silver nanowires,<sup>24</sup> (b) have semiconducting property,<sup>37</sup> (c) be used as surface coatings,<sup>220</sup> and, (d) when combined with Fmoc at its N-terminal, form Fmoc-FF hydrogels.<sup>219</sup>

Ulijn's lab showed that several terminal unprotected tripeptides KYF, KYY, KFF, and KYW selected first from the simulation and designed library ( $20^3 = 8000$  entities) can form hydrogels.<sup>46</sup> In another remarkable discovery, they found that various combinations of tripeptides containing phenylalanine and tyrosine, *e.g.*, FDY, YDF, FYD, YFD, DFY, and DYF, form various colorful pigments after enzymatic oxidation.<sup>47</sup> Hauser's lab reported several cone-shaped tripeptides that form stiff hydrogels.<sup>40</sup> Hamachi's lab reported Boolean logic gates (OR and AND) into the hydrogel–enzyme hybrid materials, which were able to sense simultaneously plural specific biochemicals and execute a controlled drug release in accordance with the logic operation.<sup>44</sup> Messersmith's lab reported that the SAP motifs containing dopamine have notable adhesion properties. They furthermore showed that polymers containing DOPA coated on nanofabricated nanopillar surfaces have both reversible wet/dry adhesion properties.<sup>31</sup>

Another class of SAPs is the lipid-like peptide that are similar to surfactants with cationic, anionic, and zwitterionic detergent properties. They have hydrophilic heads and hydrophobic tails comprised of 1–2 residues and 3–6 residues, respectively. They have been used to stabilize membrane protein production and purification, and to stabilize membrane proteins, including glycerol-3-phosphate dehydrogenase, photosystem-I (PSI), G-protein coupled receptor-bovine rhodopsin, and olfactory receptors.<sup>21,22,221–227</sup>

### 5.5. Self-Assembling Peptide Materials and Technology Used in Clinic Areas

Several chiral SAPs using D-amino acids and L-amino acids have been produced as commercial products, including Sciobio-I, -II, -III, and -IV. The success of the clinical products confirmed SAPs usefulness for clinics (Figure 14). These SAP scaffolds are



**Figure 14.** Some cases that use chiral self-assembling system technology in clinical applications. (A) Use in chronic diabetic venous ulcer (I, before treatment; 2 days after treatment; 16 days later the ulcer is healing). (B) Use in the chronic diabetic foot (I, the blood supply of the local flap was poor and necrosis occurred after amputated foot surgery; II, 20 days after treated picture; III, 87 days later and wound is healing). (C) Use in radiation ulcer (left breast) (I, the radiation ulcer cannot heal before treatment; II, 7 days after treated; III, 17 days later and radiation wound is healing). These patients are volunteers treated by Sciobio products designed by chiral self-assembling system technology (Saienbei liquid dressing). Photos are courtesy of Dr. Xia Yuping, international stoma therapist of vascular surgery, the First People's Hospital, Yibin City, China. Reproduced with permission, Dr. Xia Yuping. Copyright 2020.

approved for use in accelerated wound healing, uterine repair, myocardial infarction repair, cartilage repair, and bone repair and have been used to treat patients with severe bedsore and chronic diabetic ulcer. Although the first SAP EAK16 was initially discovered in the yeast protein Zuotin, SAPs have since been translated into a variety of clinically applicable products.

### 6. CONCLUDING REMARKS AND PERSPECTIVES

Discoveries and inventions of new materials should benefit society. It is not enough to make an exciting discovery of a new material, file a patent, publish a high-profile paper, and move on. Academic researchers should be encouraged to make their new materials widely available for others to use and make them commercially available. Since the discovery of the first self-assembling peptide scaffold hydrogels, there have been many and varied undertakings to produce various affordable commercial products on a large scale that benefit society.

In science, there are numerous examples of curiosity-driven research and unintentional discoveries that led to technological breakthroughs and new economic development. These include the mad pursuit of the DNA double-helix structure, DNA–RNA and RNA–RNA hybridizations, reverse transcription, RNA splicing, RNA as enzymes, telomeres, programmed cell death, ribosome structures, stem cells, nuclear transfer in animal

cloning, CRISPR, indispensable internet, and the World Wide Web.

The discovery of the first self-assembling peptide is no exception. It originated from making a very careful observation with curiosity and asking a seemingly simple question about what may be the structure and function of such a repetitive peptide sequence in a yeast protein. This unexpected curiosity-driven question later led to the development of SAP nanofiber scaffold hydrogel materials with wide range of uses. Thus, curiosity-driven research must be strongly encouraged and sustainably supported despite the current emphasis of application-driven research. The many aforementioned examples of various uses of SAPs all originate from asking a curious question about the peptide structure in a yeast protein.

Since then a considerable number of researchers have dedicated their careers to the SAP field and, after quite some time, SAP-based applications have been entering clinics or clinical trials. Their intrinsic nature of being self-assembling was both their blessing and their curse: being capable of making reproducible and tailorable long micro- and nanostructures with small-molecular-weight synthetic peptides was a paramount benefit. However, given the weak molecular bonds involved in the self-assembling phenomenon, most SAP scaffolds featured modest mechanical properties, making them fragile and unsuited for the regeneration of elastic tissues and for some powerful biomaterial processing technologies. That is why, in contrast to synthetic long-chain polymers, they have been mainly used as injectable fillers, substrates for *in vitro* experiments, or scaffolds for soft tissues. New venues are being explored by researchers to fill this gap, and, as already discussed, they mainly comprise additional processing of SAP scaffolds after self-assembling. Recent achievements like chemical SAP cross-linking will enlarge the number of applications of SAPs as never before, both in tissue engineering and in electronics, and will likely make them comparable and even superior to all other current biomaterials.

### APPENDIX A

#### Timeline of Self-Assembling Peptide Materials

1967: Davidson and Fasman reported poly-L-lysine undergo conformational  $\alpha$ -helix, coil, and  $\beta$ -sheet transitions.<sup>1</sup>

1973: Rippon et al. reported poly(Glu-Ala)<sub>n</sub> forming  $\beta$ -sheet with high molecular weight.<sup>2</sup>

1975: André Brack and Leslie Orgel reported poly(KV)<sub>n</sub> formed stable  $\beta$ -sheet but did not ask if the polymer formed nanofiber materials.<sup>3</sup>

1978: Goodman's lab reported various conformations of poly(Ly-Tyr)<sub>n</sub>.<sup>4</sup>

1984 Yanagawa's lab reported poly glycine sheets from repeated heating and cooling of glycinamide solution.<sup>5</sup>

1985: (i) Osterman and Kaiser reported amphiphilic  $\beta$ -structures;<sup>6</sup> (ii) Urry's lab reported poly(GVGVP)<sub>n</sub> gamma irradiation cross-linked materials.<sup>7</sup>

1990: Shuguang Zhang serendipitously discovered a self-assembling peptide in a yeast protein Zuotin.<sup>8</sup>

1993: Zhang et al. reported the discovery of a self-assembling peptide material EAK16.<sup>9</sup>

1995: Zhang et al. reported the peptide material as 3D medium for tissue cell culture.<sup>10</sup>

1997: Aggeli et al. reported another self-assembling peptide from transmembrane segment of IsK (minK) protein that formed a hydrogel.<sup>11</sup>

1999: Zhang et al. reported design surface self-assembling peptides (molecular paint) for cells to form designed specific surface patterns.<sup>12</sup>

2000: Holmes et al. reported self-assembling peptide scaffold RADA16 culture neural cells that form active synapses.<sup>13</sup>

2001: (i) Stupp's lab reported a five-part self-assembling peptide material for bone formation;<sup>14</sup> (ii) Messersmith's lab reported thermally and photochemically triggered self-assembly of peptide hydrogels.<sup>15</sup>

2002: (i) Vauthey et al.;<sup>16</sup> (ii) Santoso et al.<sup>17</sup> reported the lipid-like self-assembling peptide materials; (iii) Schneider and Pochan's lab reported pH responsive peptide hydrogel material.<sup>18</sup>

2003: (i) Reches and Gazit reported diphenylalanine (FF) form nanotube to encase silver ions;<sup>19</sup> (ii) Ryadnov and Woolfson reported  $\alpha$ -helical self-assembling protein fiber.<sup>20</sup>

2004: (i) Hamachi's lab reported the self-assembled peptide/protein array;<sup>21</sup> (ii) Messersmith's lab reported peptide-PEG conjugated materials.<sup>22</sup>

2006: (i) Gelain et al. reported self-assembling peptide materials for neural stem in 3D tissue cell cultures;<sup>23</sup> (ii) Ellis-Behnke et al. reported RADA16 scaffold repair of optical nerve of hamsters;<sup>24</sup> (iii) Ellis-Behnke et al. reported RADA16 scaffold immediate hemostasis in a few seconds in animals.<sup>25</sup>

2007: Messersmith's lab reported: (i) design a self-assembling peptide adhesive from mussel;<sup>26</sup> (ii) design wet peptide adhesives.<sup>27</sup>

2008: Zhongli Luo et al. reported chiral D-form of self-assembling peptide EAK16 that formed nanofiber scaffold materials.<sup>28,29</sup>

2009: (i) Woolfson's lab reported  $\alpha$ -helical peptide hydrogels;<sup>30</sup> (ii) Koutsopoulos et al. reported peptides scaffold hydrogel for sustained-release of proteins and monoclonal antibody.<sup>31</sup>

2010: Gazit's lab reported the optical and electronic properties of semiconductor nanocrystals of diphenylalanine (FF).<sup>32–34</sup>

2011: (i) Hauser's lab reported the cone-shaped tripeptide form stiff hydrogels;<sup>35</sup> (ii) Gelain's lab reported successfully treatment of chronically injured rat spinal cord.<sup>36</sup>

2012: (i) Gelain's lab reported discovery of new active motifs for regenerating neural cells;<sup>37</sup> (ii) Matsui's lab reported an autonomous motor of a metal-organic framework powered by reorganization of self-assembled peptides at interfaces.<sup>38</sup>

2013: Tze-wei Wang's lab reported neural stem cells encapsulated in a functionalized self-assembling peptide hydrogel for brain injury repair.<sup>39</sup>

2014: Hamachi's lab reported Boolean logic gates (OR and AND) into the hydrogel-enzyme hybrid materials.<sup>40</sup>

2015: (i) Ulijn's lab reported tripeptide self-assembled into hydrogels;<sup>41</sup> (ii) Gazit's lab reported superhelical assemblies by constrained single heptad repeat;<sup>42</sup> (iii) and light-emitting self-assembled peptide-nucleic acids.<sup>43</sup>

2016: (i) Mihara's lab reported calcium-responsive self-assembling peptides;<sup>44</sup> (ii) Świontek et al. reported a 150  $\mu\text{m}$  superhelix, the largest known helical material;<sup>45</sup> (iii) Schneider's lab reported a multiphase transitioning peptide hydrogel for suturing ultrasmall vessels;<sup>46</sup> (iv) Fan et al. reported fluorescent dipeptide nanoparticles for targeted cancer cell imaging and more;<sup>47</sup> (v) Yang's lab reported diphenylalanine peptide with controlled polarization for power generation.<sup>48</sup>

2017: Ulijn's lab reported the tripeptide with wide spectrum of colors.<sup>49</sup>

2018: (i) DeGrado's lab reported the  $\alpha$ -helical self-assembling materials;<sup>50</sup> (ii) Hamachi's lab reported an adaptive supra-molecular hydrogel;<sup>51</sup> (iii) Stupp's lab reported reversible DNA-peptide amphiphile hydrogel;<sup>52</sup> (iv) Hai Xu's lab reported nanoribbons from short peptides polar zippers between  $\beta$ -sheets.<sup>53</sup>

2019: (i) Gelain's lab reported repairing semichronic spinal injury in rats using designed self-assembling materials;<sup>54</sup> (ii) Gazit's lab reported tripeptide helical-like assemblies.<sup>55</sup>

## AUTHOR INFORMATION

### Corresponding Authors

**Shuguang Zhang** – Laboratory of Molecular Architecture, Media Lab, Massachusetts Institute of Technology, Cambridge, Massachusetts 02139-4307, United States; [orcid.org/0000-0002-3856-3752](https://orcid.org/0000-0002-3856-3752); Email: [shuguang@mit.edu](mailto:shuguang@mit.edu)

**Febrizio Gelain** – Institute for Stem-cell Biology, Regenerative Medicine and Innovative Therapies, IRCCS Casa Sollievo della Sofferenza, San Giovanni Rotondo 71013, Italy; Center for Nanomedicine and Tissue Engineering, ASST Grande Ospedale Metropolitano Niguarda, Milan 20162, Italy; [orcid.org/0000-0002-2624-5853](https://orcid.org/0000-0002-2624-5853); Email: [f.gelain@css-mendel.it](mailto:f.gelain@css-mendel.it)

**Zhongli Luo** – College of Basic Medical Sciences, Molecular Medicine and Cancer Research Center, Chongqing Medical University, Chongqing 400016, China; [orcid.org/0000-0003-4041-7807](https://orcid.org/0000-0003-4041-7807); Email: [Zhongliluo@163.com](mailto:Zhongliluo@163.com)

Complete contact information is available at:  
<https://pubs.acs.org/10.1021/acs.chemrev.0c00690>

### Author Contributions

<sup>†</sup>F.G. and Z.L. are equal first contributing authors.

### Notes

The authors declare the following competing financial interest(s): Fabrizio Gelain is a cofounder of Nanomed 3D s.r.l. (Milan, Italy) and has shares in the company. Zhongli Luo is a co-founder of Sciobio, Ltd., in Chengdu, China, and has shares in the company. Shuguang Zhang is a co-founder of 3DMatrix Inc, also a scientific advisor and has shares in the company.

### Biographies

Fabrizio Gelain has 20 years of experience in the tissue engineering and nanotech fields: he developed new functionalized SAPs and cross-linked electrospun SAPs for 3D cell cultures and neural tissue regeneration. He is Scientific Director of the Center for Nanomedicine & Tissue Engineering in Milan, Head Unit at ISBREMITE at "IRCCS Casa Sollievo della Sofferenza" hospital, formerly at the Stem Cell Research Institute (Milan), at the Center for Biomedical Engineering of the Massachusetts Institute of Technology, and at the Molecular Foundry of Lawrence Berkeley National Lab. In 2010, he cofounded Nanomed 3D, a spin-off company dedicated to the development of self-assembling biomaterials for research applications.

Zhongli Luo is a Professor at the College of Basic Medical Sciences & Molecular Medicine and Cancer Research Center at Chongqing Medical University in China. He earned his Ph.D. under the guidance by Shuguang Zhang in Biochemistry & Molecular Biology from Sichuan University of China. He published several papers in energy engineering and nanobiotechnology from designer chiral SAPs, pursue the highlight of membrane proteins, nanomedicines to clinical applications, and wound healing and tissue engineering in biomedical areas. He was a Postdoctoral Fellow under the guidance by Bengt Nordén at Chalmers

University of Technology in Sweden. Now he is a cofounder of the Sciobio Surgery Institute of Chengdu, and his studies are supported by the Natural Science Foundation Project of CQ CSTC and National Natural Science Foundation of China (NSFC).

Shuguang Zhang is at the MIT Media Lab, Massachusetts Institute of Technology. He received his B.S. from Sichuan University, China, and Ph.D. in Biochemistry and Molecular Biology from the University of California at Santa Barbara, USA. He was an American Cancer Society Postdoctoral Fellow and a Whitaker Foundation Investigator at MIT. His work of designer self-assembling peptide scaffold won the 2004 R&D100 award. He won a 2006 Guggenheim Fellowship and spent an academic sabbatical at the University of Cambridge, Cambridge, UK. He won the 2006 Wilhelm Exner Medal of Austria. He was elected to Austrian Academy of Sciences in 2010, to the American Institute of Medical and Biological Engineering in 2011, and to the U.S. National Academy of Inventors in 2013. He won the 2020 Emil Thomas Kaiser Award from the Protein Society. He published >170 scientific papers that have been cited over 32 000 times with an h-index of 85. He is also a cofounder and board member of Molecular Frontiers Foundation that organizes annually Molecular Frontiers Symposia in Sweden and around the world. The Foundation encourages young people to ask good scientific questions about nature. The selected winners will be awarded for Molecular Frontiers Inquiry Prize.

## ACKNOWLEDGMENTS

Zhongli Luo was supported by the grant from the National Natural Science Foundation of China (project nos. NSFC 31771101 and 31540019), the Natural Science Foundation of CQ CSTC (Key) under grant (project no. CSTC2015JCYJBX0072). Fabrizio Gelain was supported by the “Ricerca Corrente 2018–2020” funding granted by the Italian Ministry of Health, by the “5x1.000” voluntary contributions and by Revert Onlus. We gratefully acknowledge Dorrie Langsley for careful and dedicated editing and making many constructive suggestions to significantly improve this review.

## ABBREVIATIONS

3D = three dimensions  
 BDNF = brain derived neurotrophic factor  
 bFGF = basic fibroblast growth factor  
 BMP-2 = bone morphogenetic protein 2  
 BSA = bovine serum albumin  
 CAP = co-assembling peptide  
 CD = circular dichroism  
 CNS = central nervous system  
 ECM = extracellular matrix  
 FAQ = FAQRVPP functional motif fostering hNSC differentiation  
 FF = phenylalanine–phenylalanine  
 GPa = giga Pascal  
 HA = hydroxyapatite  
 IGF-1 = insulin-like growth factor 1  
 IHD = ischemic heart disease  
 iPSCs = induced pluripotent stem cells  
 KPa = kilo Pascal  
 MMP = matrix metalloproteinase  
 MSC = mesenchymal stem cells  
 NGF = nerve growth factor  
 NPC = neural progenitor cell  
 NSC = neural stem cells  
 OA = osteoarthritis

Pa = Pascal  
 PA = peptide amphiphile  
 PEG = polyethylene glycol  
 PSI = photosystem-I  
 PCL = polycaprolactone  
 PLGA = poly(lactic-co-glycolic acid)  
 PLLA = poly-L-lactic acid  
 PNT = peripheral nerve transections  
 pPAK = p21-activated kinase  
 SAP = self-assembling peptides  
 SCI = spinal cord injuries  
 SEM = scanning electron microscope  
 sulfo-SMCC = sulfosuccinimidyl 4-(N-maleimidomethyl)-cyclohexane-1-carboxylate  
 TGF $\beta$  = transforming growth factor  $\beta$   
 $\beta$ TUB =  $\beta$  tubulin  
 VEGF = vascular endothelial growth factor

## REFERENCES

- (1) Davidson, B.; Fasman, G. D. The conformational transitions of uncharged poly-L-lysine.  $\alpha$  helix-random coil- $\beta$  structure. *Biochemistry* **1967**, *6*, 1616–1629.
- (2) Bippon, W. B.; Chen, H. H.; Walton, A. G. Spectroscopic characterization of poly(Glu-Ala). *J. Mol. Biol.* **1973**, *75*, 369–375.
- (3) Brack, A.; Orgel, L. E. Beta structures of alternating polypeptides and their possible prebiotic significance. *Nature* **1975**, *256*, 383–387.
- (4) St Pierre, S.; Ingwall, R. T.; Verlander, M. S.; Goodman, M. Conformational studies of sequential polypeptides containing lysine and tyrosine. *Biopolymers* **1978**, *17*, 1837–1848.
- (5) Yanagawa, H.; Nishizawa, M.; Kojima, K. A possible prebiotic peptide formation from glycinamide and related compounds. *Origins Life* **1984**, *14*, 267–272.
- (6) Osterman, D. G.; Kaiser, E. T. Design and characterization of peptides with amphiphilic beta-strand structures. *J. Cell. Biochem.* **1985**, *29*, 57–72.
- (7) Wood, S. A.; Prasad, K. U.; Urry, D. W. Cross-linked polypentapeptide of elastin as a calcifiable matrix: molecular weight dependence. *Calcif. Tissue Int.* **1985**, *37*, 565–571.
- (8) Zhang, S.; Lockshin, C.; Herbert, A.; Winter, E.; Rich, A. ZuoTin, a putative Z-DNA binding protein in *Saccharomyces cerevisiae*. *EMBO J.* **1992**, *11*, 3787–3796.
- (9) Zhang, S.; Holmes, T.; Lockshin, C.; Rich, A. Spontaneous assembly of a self-complementary oligopeptide to form a stable macroscopic membrane. *Proc. Natl. Acad. Sci. U. S. A.* **1993**, *90*, 3334–3338.
- (10) Zhang, S.; Holmes, T. C.; DiPersio, C. M.; Hynes, R. O.; Su, X.; Rich, A. Self-complementary oligopeptide matrices support mammalian cell attachment. *Biomaterials* **1995**, *16*, 1385–1393.
- (11) Aggeli, A.; Bell, M.; Boden, N.; Keen, J. N.; Knowles, P. F.; McLeish, T. C.; Pitkeathly, M.; Radford, S. E. Responsive gels formed by the spontaneous self-assembly of peptides into polymeric beta-sheet tapes. *Nature* **1997**, *386*, 259–262.
- (12) Zhang, S. G.; Yan, L.; Altman, M.; Lassle, M.; Nugent, H.; Frankel, F.; Lauffenburger, D. A.; Whitesides, G. M.; Rich, A. Biological surface engineering: a simple system for cell pattern formation. *Biomaterials* **1999**, *20*, 1213–1220.
- (13) Holmes, T. C.; de Lacalle, S.; Su, X.; Liu, G.; Rich, A.; Zhang, S. Extensive neurite outgrowth and active synapse formation on self-assembling peptide scaffolds. *Proc. Natl. Acad. Sci. U. S. A.* **2000**, *97*, 6728–6733.
- (14) Hartgerink, J. D.; Beniash, E.; Stupp, S. I. Self-assembly and mineralization of peptide-amphiphile nanofibers. *Science* **2001**, *294*, 1684–1688.
- (15) Collier, J. H.; Hu, B. H.; Ruberti, J. W.; Zhang, J.; Shum, P.; Thompson, D. H.; Messersmith, P. B. Thermally and photochemically triggered self-assembly of peptide hydrogels. *J. Am. Chem. Soc.* **2001**, *123*, 9463–9464.

- (16) Vauthey, S.; Santoso, S.; Gong, H. Y.; Watson, N.; Zhang, S. G. Molecular self-assembly of surfactant-like peptides to form nanotubes and nanovesicles. *Proc. Natl. Acad. Sci. U. S. A.* **2002**, *99*, 5355–5360.
- (17) Santoso, S.; Hwang, W.; Hartman, H.; Zhang, S. Self-assembly of surfactant-like peptides with variable glycine tails to form nanotubes and nanovesicles. *Nano Lett.* **2002**, *2*, 687–691.
- (18) Schneider, J. P.; Pochan, D. J.; Ozbas, B.; Rajagopal, K.; Pakstis, L.; Kretsinger, J. Responsive hydrogels from the intramolecular folding and self-assembly of a designed peptide. *J. Am. Chem. Soc.* **2002**, *124* (50), 15030–15037.
- (19) Reches, M.; Gazit, E. Casting metal nanowires within discrete self-assembled peptide nanotubes. *Science* **2003**, *300*, 625–627.
- (20) Ryadnov, M. G.; Woolfson, D. N. Engineering the morphology of a self-assembling protein fibre. *Nat. Mater.* **2003**, *2*, 329–332.
- (21) Kiyonaka, S.; Sada, K.; Yoshimura, I.; Shinkai, S.; Kato, N.; Hamachi, I. Semi-wet peptide/protein array using supramolecular hydrogel. *Nat. Mater.* **2004**, *3*, 58–64.
- (22) Collier, J. H.; Messersmith, P. B. Self-assembling polymer-peptide conjugates: nanostructural tailoring. *Adv. Mater.* **2004**, *16*, 907–910.
- (23) Gelain, F.; Bottai, D.; Vescovi, A.; Zhang, S. Designer self-assembling peptide nanofiber scaffolds for adult mouse neural stem cell 3-dimensional cultures. *PLoS One* **2006**, *1*, No. e119.
- (24) Ellis-Behnke, R. G.; Liang, Y. X.; You, S. W.; Tay, D. K.; Zhang, S.; So, K. F.; Schneider, G. E. Nano neuro knitting: peptide nanofiber scaffold for brain repair and axon regeneration with functional return of vision. *Proc. Natl. Acad. Sci. U. S. A.* **2006**, *103*, 5054–5059.
- (25) Ellis-Behnke, R. G.; Liang, Y. X.; Tay, D. K.; Kau, P. W.; Schneider, G. E.; Zhang, S.; Wu, W.; So, K. F. Nano hemostat solution: immediate hemostasis at the nanoscale. *Nanomedicine* **2006**, *2*, 207–215.
- (26) Lee, H.; Lee, B. P.; Messersmith, P. B. A Reversible wet/dry adhesive inspired by mussels and geckos. *Nature* **2007**, *448*, 338–341.
- (27) Lee, H.; Dellatore, S. M.; Miller, W. M.; Messersmith, P. B. Mussel-inspired surface chemistry for multifunctional coatings. *Science* **2007**, *318*, 426–430.
- (28) Luo, Z.; Zhao, X.; Zhang, S. Structural dynamic of a self-assembling peptide d-EAK16 made of only d-amino acids. *PLoS One* **2008**, *3*, No. e2364.
- (29) Luo, Z.; Zhao, X.; Zhang, S. Self-organization of a chiral d-EAK16 designer peptide into a 3d nanofiber scaffold. *Macromol. Biosci.* **2008**, *8*, 785–791.
- (30) Banwell, E. F.; Abelardo, E. S.; Adams, D. J.; Birchall, M. A.; Corrigan, A.; Donald, A. M.; Kirkland, M.; Serpell, L. C.; Butler, M. F.; Woolfson, D. N. Rational design and application of responsive alpha-helical peptide hydrogels. *Nat. Mater.* **2009**, *8*, 596–600.
- (31) Koutsopoulos, S.; Unsworth, L. D.; Nagai, Y.; Zhang, S. Controlled release of functional proteins through designer self-assembling peptide nanofiber hydrogel scaffold. *Proc. Natl. Acad. Sci. U. S. A.* **2009**, *106*, 4623–4628.
- (32) Amdursky, N.; Molotskii, M.; Gazit, E.; Rosenman, G. Elementary building blocks of self-assembled peptide nanotubes. *J. Am. Chem. Soc.* **2010**, *132*, 15632–15636.
- (33) Amdursky, N.; Beker, P.; Schklovsky, J.; Gazit, E.; Rosenman, G. Ferroelectric and related phenomena in biological and bioinspired nanostructures. *Ferroelectrics* **2010**, *399*, 107–117.
- (34) Amdursky, N.; Gazit, E.; Rosenman, G. Quantum confinement in self-assembled bioinspired peptide hydrogels. *Adv. Mater.* **2010**, *22*, 2311–2315.
- (35) Hauser, C. A.; Deng, R.; Mishra, A.; Loo, Y.; Khoe, U.; Zhuang, F.; Cheong, D. W.; Accardo, A.; Sullivan, M. B.; Riekel, C.; et al. Natural tri- to hexapeptides self-assemble in water to amyloid beta-type fiber aggregates by unexpected alpha-helical intermediate structures. *Proc. Natl. Acad. Sci. U. S. A.* **2011**, *108*, 1361–1366.
- (36) Gelain, F.; Panseri, S.; Antonini, S.; Cunha, C.; Donega, M.; Lowery, J.; Taraballi, F.; Cerri, G.; Montagna, M.; Baldissera, F.; et al. Transplantation of nanostructured composite scaffolds results in the regeneration of chronically injured spinal cords. *ACS Nano* **2011**, *5*, 227–236.
- (37) Gelain, F.; Cigognini, D.; Caprini, A.; Silva, D.; Colleoni, B.; Donega, M.; Antonini, S.; Cohen, B. E.; Vescovi, A. New bioactive motifs and their use in functionalized self-assembling peptides for NSC differentiation and neural tissue engineering. *Nanoscale* **2012**, *4*, 2946–2957.
- (38) Ikezoe, Y.; Washino, G.; Uemura, T.; Kitagawa, S.; Matsui, H. Autonomous motors of a metal-organic framework powered by reorganization of self-assembled peptides at interfaces. *Nat. Mater.* **2012**, *11*, 1081–1085.
- (39) Cheng, T. Y.; Chen, M. H.; Chang, W. H.; Huang, M. Y.; Wang, T. W. Neural stem cells encapsulated in a functionalized self-assembling peptide hydrogel for brain tissue engineering. *Biomaterials* **2013**, *34*, 2005–2016.
- (40) Ikeda, M.; Tanida, T.; Yoshii, T.; Kurotani, K.; Onogi, S.; Urayama, K.; Hamachi, I. Installing logic-gate responses to a variety of biological substances in supramolecular hydrogel-enzyme hybrids. *Nat. Chem.* **2014**, *6*, 511–518.
- (41) Frederix, P. W.; Scott, G. G.; Abul-Haija, Y. M.; Kalafatovic, D.; Pappas, C. G.; Javid, N.; Hunt, N. T.; Ulijn, R. V.; Tuttle, T. Exploring the sequence space for (tri-)peptide self-assembly to design and discover new hydrogels. *Nat. Chem.* **2015**, *7*, 30–37.
- (42) Mondal, S.; Adler-Abramovich, L.; Lampel, A.; Bram, Y.; Lipstman, S.; Gazit, E. Formation of functional super-helical assemblies by constrained single heptad repeat. *Nat. Commun.* **2015**, *6*, 8615.
- (43) Berger, O.; Adler-Abramovich, L.; Levy-Sakin, M.; Grunwald, A.; Liebes-Peer, Y.; Bachar, M.; Buzhansky, L.; Mossou, E.; Forsyth, V. T.; Schwartz, T.; et al. Light-emitting self-assembled peptide nucleic acids exhibit both stacking interactions and Watson-Crick base pairing. *Nat. Nanotechnol.* **2015**, *10*, 353–360.
- (44) Fukunaga, K.; Tsutsumi, H.; Mihara, H. Cell differentiation on disk- and string-shaped hydrogels fabricated from Ca<sup>2+</sup>-responsive self-assembling peptides. *Biopolymers* **2016**, *106*, 476–483.
- (45) Świontek, M.; Kaminski, Z. J.; Kolesinska, B.; Seebach, D. Visible-light microscopic discovery of up to 150 μm long helical amyloid fibrils built of the dodecapeptide H-(Val-Ala-Leu)<sub>4</sub>-OH and of decapeptides derived from insulin. *Chem. Biodiversity* **2016**, *13*, 1111–1117.
- (46) Smith, D. J.; Brat, G. A.; Medina, S. H.; Tong, D.; Huang, Y.; Grahmmer, J.; Furtmuller, G. J.; Oh, B. C.; Nagy-Smith, K. J.; Walczak, P.; et al. A multiphase transitioning peptide hydrogel for suturing ultrasmall vessels. *Nat. Nanotechnol.* **2016**, *11*, 95–102.
- (47) Fan, Z.; Sun, L. M.; Huang, Y. J.; Wang, Y. Z.; Zhang, M. J. Bioinspired fluorescent dipeptide nanoparticles for targeted cancer cell imaging and real-time monitoring of drug release. *Nat. Nanotechnol.* **2016**, *11*, 388.
- (48) Nguyen, V.; Zhu, R.; Jenkins, K.; Yang, R. Self-assembly of diphenylalanine peptide with controlled polarization for power generation. *Nat. Commun.* **2016**, *7*, 13566.
- (49) Lampel, A.; McPhee, S. A.; Park, H. A.; Scott, G. G.; Humagain, S.; Hekstra, D. R.; Yoo, B.; Frederix, P.; Li, T. D.; Abzalimov, R. R.; et al. Polymeric peptide pigments with sequence-encoded properties. *Science* **2017**, *356*, 1064–1068.
- (50) Zhang, S. Q.; Huang, H.; Yang, J.; Kratochvil, H. T.; Lolicato, M.; Liu, Y.; Shu, X.; Liu, L.; DeGrado, W. F. Designed peptides that assemble into cross-alpha amyloid-like structures. *Nat. Chem. Biol.* **2018**, *14*, 870–875.
- (51) Shigemitsu, H.; Fujisaku, T.; Tanaka, W.; Kubota, R.; Minami, S.; Urayama, K.; Hamachi, I. An Adaptive supramolecular hydrogel comprising self-sorting double nanofiber networks. *Nat. Nanotechnol.* **2018**, *13*, 165–172.
- (52) Freeman, R.; Han, M.; Alvarez, Z.; Lewis, J. A.; Wester, J. R.; Stephanopoulos, N.; McClendon, M. T.; Lynsky, C.; Godbe, J. M.; Sangji, H.; et al. Reversible self-assembly of superstructured networks. *Science* **2018**, *362*, 808–813.
- (53) Wang, M.; Wang, J.; Zhou, P.; Deng, J.; Zhao, Y.; Sun, Y.; Yang, W.; Wang, D.; Li, Z.; Hu, X.; et al. Nanoribbons self-assembled from short peptides demonstrate the formation of polar zippers between beta-sheets. *Nat. Commun.* **2018**, *9*, 5118.

- (54) Marchini, A.; Raspa, A.; Pugliese, R.; El Malek, M. A.; Pastori, V.; Lecchi, M.; Vescovi, A. L.; Gelain, F. Multifunctionalized hydrogels foster hnsC maturation in 3d cultures and neural regeneration in spinal cord injuries. *Proc. Natl. Acad. Sci. U. S. A.* **2019**, *116*, 7483–7492.
- (55) Bera, S.; Mondal, S.; Xue, B.; Shimon, L. J. W.; Cao, Y.; Gazit, E. Rigid helical-like assemblies from a self-aggregating tripeptide. *Nat. Mater.* **2019**, *18*, 503–509.
- (56) Zhang, S.; Altman, M. Peptide self-assembly in functional polymer science and engineering. *React. Funct. Polym.* **1999**, *41*, 91–102.
- (57) Zhang, S. Fabrication of novel biomaterials through molecular self-assembly. *Nat. Biotechnol.* **2003**, *21*, 1171–1178.
- (58) Firth, A.; Aggeli, A.; Burke, J. L.; Yang, X.; Kirkham, J. Biomimetic self-assembling peptides as injectable scaffolds for hard tissue engineering. *Nanomedicine (London, U. K.)* **2006**, *1*, 189–199.
- (59) Gazit, E. Self-Assembled Peptide Nanostructures: The design of molecular building blocks and their technological utilization. *Chem. Soc. Rev.* **2007**, *36*, 1263–1269.
- (60) Ulijn, R. V.; Smith, A. M. Designing peptide-based nanomaterials. *Chem. Soc. Rev.* **2008**, *37*, 664–675.
- (61) Zhang, S. Emerging biological materials through molecular self-assembly. *Biotechnol. Adv.* **2002**, *20*, 321–339.
- (62) Zhang, S. Beyond the petri dish. *Nat. Biotechnol.* **2004**, *22*, 151–152.
- (63) Kyle, S.; Aggeli, A.; Ingham, E.; McPherson, M. J. Production of self-assembling biomaterials for tissue engineering. *Trends Biotechnol.* **2009**, *27*, 423–433.
- (64) Adler-Abramovich, L.; Gazit, E. The physical properties of supramolecular peptide assemblies: from building block association to technological applications. *Chem. Soc. Rev.* **2014**, *43*, 6881–6893.
- (65) Luo, Z.; Zhang, S. Designer nanomaterials using chiral self-assembling peptide systems and their emerging benefit for society. *Chem. Soc. Rev.* **2012**, *41*, 4736–4754.
- (66) Pugliese, R.; Gelain, F. Peptidic biomaterials: from self-assembling to regenerative medicine. *Trends Biotechnol.* **2017**, *35*, 145–158.
- (67) Tao, K.; Makam, P.; Aizen, R.; Gazit, E. Self-assembling peptide semiconductors. *Science* **2017**, *358*, No. eaam9756, (pp.1–7)..
- (68) Zhang, S. Discovery and design of self-assembling peptides. *Interface Focus* **2017**, *7*, 20170028.
- (69) Regan, L.; DeGrado, W. F. Characterization of a helical protein designed from first principles. *Science* **1988**, *241*, 976–978.
- (70) Kamtekar, S.; Schiffer, J. M.; Xiong, H.; Babik, J. M.; Hecht, M. H. Protein design by binary patterning of polar and nonpolar amino acids. *Science* **1993**, *262*, 1680–1685.
- (71) Petka, W. A.; Harden, J. L.; McGrath, K. P.; Wirtz, D.; Tirrell, D. A. Reversible hydrogels from self-assembling artificial proteins. *Science* **1998**, *281*, 389–392.
- (72) Kim, U. J.; Park, J.; Li, C.; Jin, H. J.; Valluzzi, R.; Kaplan, D. L. Structure and properties of silk hydrogels. *Biomacromolecules* **2004**, *5*, 786–792.
- (73) Olsen, B. D.; Kornfield, J. A.; Tirrell, D. A. Yielding behavior in injectable hydrogels from telechelic proteins. *Macromolecules* **2010**, *43*, 9094–9099.
- (74) Jonker, A. M.; Löwik, D. W. P. M.; van Hest, J. C. M. Peptide- and protein-based hydrogels. *Chem. Mater.* **2012**, *24*, 759–773.
- (75) Tang, S.; Glassman, M. J.; Li, S.; Socrate, S.; Olsen, B. D. Oxidatively responsive chain extension to entangle engineered protein hydrogels. *Macromolecules* **2014**, *47*, 791–799.
- (76) Schloss, A. C.; Williams, D. M.; Regan, L. J. Protein-based hydrogels for tissue engineering. *Adv. Exp. Med. Biol.* **2016**, *940*, 167–177.
- (77) Rapp, P. B.; Omar, A. K.; Shen, J. J.; Buck, M. E.; Wang, Z. G.; Tirrell, D. A. Analysis and control of chain mobility in protein hydrogels. *J. Am. Chem. Soc.* **2017**, *139*, 3796–3804.
- (78) Wu, J.; et al. Rationally designed synthetic protein hydrogels with predictable mechanical properties. *Nat. Commun.* **2018**, *9*, 620.
- (79) Zhang, S.; Rich, A. Direct conversion of an oligopeptide from a beta-sheet to an alpha-helix: a model for amyloid formation. *Proc. Natl. Acad. Sci. U. S. A.* **1997**, *94*, 23–28.
- (80) Altman, M.; Lee, P.; Rich, A.; Zhang, S. Conformational behavior of ionic self-complementary peptides. *Protein Sci.* **2000**, *9*, 1095–1105.
- (81) Caplan, M. R.; Moore, P. N.; Zhang, S.; Kamm, R. D.; Lauffenburger, D. A. Self-assembly of a beta-sheet protein governed by relief of electrostatic repulsion relative to van der Waals attraction. *Biomacromolecules* **2000**, *1*, 627–631.
- (82) Caplan, M. R.; Schwartzfarb, E. M.; Zhang, S.; Kamm, R. D.; Lauffenburger, D. A. Control of self-assembling oligopeptide matrix formation through systematic variation of amino acid sequence. *Biomaterials* **2002**, *23*, 219–227.
- (83) Caplan, M. R.; Schwartzfarb, E. M.; Zhang, S.; Kamm, R. D.; Lauffenburger, D. A. Effects of systematic variation of amino acid sequence on the mechanical properties of a self-assembling, oligopeptide biomaterial. *J. Biomater. Sci., Polym. Ed.* **2002**, *13*, 225–236.
- (84) Collins, J. M.; Singh, S. K.; Porter, K. A.; Karney, M. J. Pushing the limits of peptide synthesis further. *J. Pept. Sci.* **2014**, *20*, S51–S51.
- (85) Porter, K. A.; Singh, S. K.; Collins, J. M. High throughput sequential peptide synthesis with high efficiency solid phase peptide synthesis (He-Spps). *J. Pept. Sci.* **2014**, *20*, S150–S151.
- (86) Taraballi, F.; Natalello, A.; Campione, M.; Villa, O.; Doglia, S. M.; Paleari, A.; Gelain, F. Glycine-spacers influence functional motifs exposure and self-assembling propensity of functionalized substrates tailored for neural stem cell cultures. *Front. Neuroeng.* **2010**, *3*, 1.
- (87) Anderson, J. M.; Andukuri, A.; Lim, D. J.; Jun, H. W. Modulating the gelation properties of self-assembling peptide amphiphiles. *ACS Nano* **2009**, *3*, 3447–3454.
- (88) Guttenplan, A. P. M.; Young, L. J.; Matak-Vinkovic, D.; Kaminski, C. F.; Knowles, T. P. J.; Itzhaki, L. S. Nanoscale click-reactive scaffolds from peptide self-assembly. *J. Nanobiotechnol.* **2017**, *15*, 70.
- (89) Mahmoud, Z. N.; Gunnoo, S. B.; Thomson, A. R.; Fletcher, J. M.; Woolfson, D. N. Bioorthogonal dual functionalization of self-assembling peptide fibers. *Biomaterials* **2011**, *32*, 3712–3720.
- (90) Gray, B. P.; Brown, K. C. Combinatorial peptide libraries: mining for cell-binding peptides. *Chem. Rev.* **2014**, *114*, 1020–1081.
- (91) Li, Y.; Liu, X.; Dong, X.; Zhang, L.; Sun, Y. Biomimetic design of affinity peptide ligand for capsomere of virus-like particle. *Langmuir* **2014**, *30*, 8500–8508.
- (92) Horii, A.; Wang, X.; Gelain, F.; Zhang, S. Biological designer self-assembling peptide nanofiber scaffolds significantly enhance osteoblast proliferation, differentiation and 3D migration. *PLoS One* **2007**, *2*, No. e190.
- (93) Danesin, R.; Brun, P.; Roso, M.; Delaunay, F.; Samouillan, V.; Brunelli, K.; Iucci, G.; Ghezzi, F.; Modesti, M.; Castagliuolo, I.; et al. Self-assembling peptide-enriched electrospun polycaprolactone scaffolds promote the h-osteoblast adhesion and modulate differentiation-associated gene expression. *Bone* **2012**, *51*, 851–859.
- (94) Yan, M.; Lewis, P. L.; Shah, R. N. Tailoring nanostructure and bioactivity of 3D-printable hydrogels with self-assemble peptides amphiphile for promoting bile duct formation. *Biofabrication* **2018**, *10*, 035010.
- (95) Ceylan, H.; Kocabey, S.; Unal Gulsuner, H.; Balci, O. S.; Guler, M. O.; Tekinay, A. B. Bone-like mineral nucleating peptide nanofibers induce differentiation of human mesenchymal stem cells into mature osteoblasts. *Biomacromolecules* **2014**, *15*, 2407–2418.
- (96) Ustun Yaylaci, S.; Sardan Ekiz, M.; Arslan, E.; Can, N.; Kilic, E.; Ozkan, H.; Orujalipoor, I.; Ide, S.; Tekinay, A. B.; Guler, M. O. Supramolecular gag-like self-assembled glycopeptide nanofibers induce chondrogenesis and cartilage regeneration. *Biomacromolecules* **2016**, *17*, 679–689.
- (97) Anderson, J. M.; Vines, J. B.; Patterson, J. L.; Chen, H.; Javed, A.; Jun, H. W. Osteogenic differentiation of human mesenchymal stem cells synergistically enhanced by biomimetic peptide amphiphiles combined with conditioned medium. *Acta Biomater.* **2011**, *7*, 675–682.
- (98) Shah, R. N.; Shah, N. A.; Del Rosario Lim, M. M.; Hsieh, C.; Nuber, G.; Stupp, S. I. Supramolecular design of self-assembling

nanofibers for cartilage regeneration. *Proc. Natl. Acad. Sci. U. S. A.* **2010**, *107*, 3293–3298.

(99) Li, R.; Xu, J.; Wong, D. S. H.; Li, J.; Zhao, P.; Bian, L. Self-assembled n-cadherin mimetic peptide hydrogels promote the chondrogenesis of mesenchymal stem cells through inhibition of canonical Wnt/Beta-catenin signaling. *Biomaterials* **2017**, *145*, 33–43.

(100) Boopathy, A. V.; Martinez, M. D.; Smith, A. W.; Brown, M. E.; Garcia, A. J.; Davis, M. E. Intramyocardial delivery of Notch ligand-containing hydrogels improves cardiac function and angiogenesis following infarction. *Tissue Eng., Part A* **2015**, *21*, 2315–2322.

(101) Boopathy, A. V.; Che, P. L.; Somasuntharam, I.; Fiore, V. F.; Cabigas, E. B.; Ban, K.; Brown, M. E.; Narui, Y.; Barker, T. H.; Yoon, Y. S.; et al. The modulation of cardiac progenitor cell function by hydrogel-dependent Notch1 activation. *Biomaterials* **2014**, *35*, 8103–8112.

(102) Numata, K.; Hamasaki, J.; Subramanian, B.; Kaplan, D. L. Gene delivery mediated by recombinant silk proteins containing cationic and cell binding motifs. *J. Controlled Release* **2010**, *146*, 136–143.

(103) Nowakowski, G. S.; Dooner, M. S.; Valinski, H. M.; Mihaliak, A. M.; Quesenberry, P. J.; Becker, P. S. A specific heptapeptide from a phage display peptide library homes to bone marrow and binds to primitive hematopoietic stem cells. *Stem Cells* **2004**, *22*, 1030–1038.

(104) Gelain, F.; Silva, D.; Caprini, A.; Taraballi, F.; Natalello, A.; Villa, O.; Nam, K. T.; Zuckermann, R. N.; Doglia, S. M.; Vescovi, A. BMHP1-derived self-assembling peptides: hierarchically assembled structures with self-healing propensity and potential for tissue engineering applications. *ACS Nano* **2011**, *5*, 1845–1859.

(105) Caprini, A.; Silva, D.; Zanoni, I.; Cunha, C.; Volonte, C.; Vescovi, A.; Gelain, F. A novel bioactive peptide: assessing its activity over murine neural stem cells and its potential for neural tissue engineering. *New Biotechnol.* **2013**, *30*, 552–562.

(106) Sawada, T.; Mihara, H. Dense surface functionalization using peptides that recognize differences in organized structures of self-assembling nanomaterials. *Mol. BioSyst.* **2012**, *8*, 1264–1274.

(107) Jin, H. E.; Jang, J.; Chung, J.; Lee, H. J.; Wang, E.; Lee, S. W.; Chung, W. J. Biomimetic self-templated hierarchical structures of collagen-like peptide amphiphiles. *Nano Lett.* **2015**, *15*, 7138–7145.

(108) Seki, T.; So, C. R.; Page, T. R.; Starkebaum, D.; Hayamizu, Y.; Sarikaya, M. Electrochemical control of peptide self-organization on atomically flat solid surfaces: a case study with graphite. *Langmuir* **2018**, *34*, 1819–1826.

(109) Okur, Z.; Senturk, O. I.; Yilmaz, C.; Gulseren, G.; Mammadov, B.; Guler, M. O.; Tekinay, A. B. Promotion of neurite outgrowth by rationally designed NGF-beta binding peptide nanofibers. *Biomater. Sci.* **2018**, *6*, 1777–1790.

(110) Taraballi, F.; Campione, M.; Vescovi, A.; Sassella, A.; Paleari, A.; Hwang, W.; Gelain, F. Effect of functionalization on the self-assembling propensity of  $\beta$ -sheet forming peptides. *Soft Matter* **2009**, *5*, 660–668.

(111) Raspa, A.; Saracino, G. A. A.; Pugliese, R.; Silva, D.; Cigognini, D.; Vescovi, A.; Gelain, F. Complementary co-assembling peptides: from in silico studies to in vivo application. *Adv. Funct. Mater.* **2014**, *24*, 6317–6328.

(112) Silva, D.; Natalello, A.; Sanii, B.; Vasita, R.; Saracino, G.; Zuckermann, R. N.; Doglia, S. M.; Gelain, F. Synthesis and characterization of designed BMHP1-derived self-assembling peptides for tissue engineering applications. *Nanoscale* **2013**, *5*, 704–718.

(113) Engler, A. J.; Sen, S.; Sweeney, H. L.; Discher, D. E. Matrix elasticity directs stem cell lineage specification. *Cell* **2006**, *126*, 677–689.

(114) Bartlett, R. D.; Choi, D.; Phillips, J. B. Biomechanical properties of the spinal cord: implications for tissue engineering and clinical translation. *Regener. Med.* **2016**, *11*, 659–673.

(115) Oftadeh, R.; Perez-Viloria, M.; Villa-Camacho, J. C.; Vaziri, A.; Nazarian, A. Biomechanics and mechanobiology of trabecular bone: a review. *J. Biomech. Eng.* **2015**, *137*, BIO-14-1365.

(116) Cunha, C.; Panseri, S.; Villa, O.; Silva, D.; Gelain, F. 3D culture of adult mouse neural stem cells within functionalized self-assembling peptide scaffolds. *Int. J. Nanomed.* **2011**, *6*, 943–955.

(117) Yokoi, H.; Kinoshita, T.; Zhang, S. Dynamic reassembly of peptide RADA16 nanofiber scaffold. *Proc. Natl. Acad. Sci. U. S. A.* **2005**, *102*, 8414–8419.

(118) Pugliese, R.; Marchini, A.; Saracino, G. A. A.; Zuckermann, R. N.; Gelain, F. Cross-linked self-assembling peptide scaffolds. *Nano Res.* **2018**, *11*, 586–602.

(119) Pugliese, R.; Maleki, M.; Zuckermann, R. N.; Gelain, F. Self-assembling peptides cross-linked with genipin: resilient hydrogels and self-standing electrospun scaffolds for tissue engineering applications. *Biomater. Sci.* **2019**, *7*, 76–91.

(120) Gelain, F.; Unsworth, L.; Zhang, S. Slow and sustained release of active cytokines from designer self-assembling peptide nanofiber scaffolds for adult mouse neural stem cell cultures. *J. Controlled Release* **2010**, *145*, 231–239.

(121) Harrington, D. A.; Cheng, E. Y.; Guler, M. O.; Lee, L. K.; Donovan, J. L.; Claussen, R. C.; Stupp, S. I. Branched peptide-amphiphiles as self-assembling coatings for tissue engineering scaffolds. *J. Biomed. Mater. Res., Part A* **2006**, *78A*, 157–167.

(122) Chen, C.; Gu, Y.; Deng, L.; Han, S.; Sun, X.; Chen, Y.; Lu, J. R.; Xu, H. Tuning gelation kinetics and mechanical rigidity of beta-hairpin peptide hydrogels via hydrophobic amino acid substitutions. *ACS Appl. Mater. Interfaces* **2014**, *6*, 14360–14368.

(123) Pugliese, R.; Fontana, F.; Marchini, A.; Gelain, F. Branched peptides integrate into self-assembled nanostructures and enhance biomechanics of peptidic hydrogels. *Acta Biomater.* **2018**, *66*, 258–271.

(124) Taraballi, F.; Campione, M.; Vescovi, A. L.; Sassella, A.; Paleari, A.; Hwang, W.; Gelain, F. Effect of functionalization on the self-assembling propensity of  $\beta$ -sheet forming peptides. *Soft Matter* **2009**, *5*, 660–668.

(125) Ibusuki, S.; Halbesma, G. J.; Randolph, M. A.; Redmond, R. W.; Kochevar, I. E.; Gill, T. J. Photochemically cross-linked collagen gels as three-dimensional scaffolds for tissue engineering. *Tissue Eng.* **2007**, *13*, 1995–2001.

(126) Ma, L.; Gao, C.; Mao, Z.; Zhou, J.; Shen, J.; Hu, X.; Han, C. Collagen/chitosan porous scaffolds with improved biostability for skin tissue engineering. *Biomaterials* **2003**, *24*, 4833–4841.

(127) Oryan, A.; Kamali, A.; Moshiri, A.; Baharvand, H.; Daemi, H. Chemical crosslinking of biopolymeric scaffolds: current knowledge and future directions of crosslinked engineered bone scaffolds. *Int. J. Biol. Macromol.* **2018**, *107*, 678–688.

(128) Chronopoulou, L.; Toumia, Y.; Cerroni, B.; Pandolfi, D.; Paradossi, G.; Palocci, C. Biofabrication of genipin-crosslinked peptide hydrogels and their use in the controlled delivery of naproxen. *New Biotechnol.* **2017**, *37*, 138–143.

(129) Maleki, M.; Natalello, A.; Pugliese, R.; Gelain, F. Fabrication of nanofibrous electrospun scaffolds from a heterogeneous library of co- and self-assembling peptides. *Acta Biomater.* **2017**, *51*, 268–278.

(130) Adler-Abramovich, L.; Aronov, D.; Beker, P.; Yevnin, M.; Stempler, S.; Buzhansky, L.; Rosenman, G.; Gazit, E. Self-Assembled arrays of peptide nanotubes by vapour deposition. *Nat. Nanotechnol.* **2009**, *4*, 849–854.

(131) Ryu, J.; Park, C. B. High-temperature self-assembly of peptides into vertically well-aligned nanowires by aniline vapor. *Adv. Mater.* **2008**, *20*, 3754–3758.

(132) Zhao, Z.; Matsui, H. Accurate immobilization of antibody-functionalized peptide nanotubes on protein-patterned arrays by optimizing their ligand-receptor interactions. *Small* **2007**, *3*, 1390–1393.

(133) Stroumpoulis, D.; Zhang, H.; Rubalcava, L.; Gliem, J.; Tirrell, M. Cell adhesion and growth to peptide-patterned supported lipid membranes. *Langmuir* **2007**, *23*, 3849–3856.

(134) Zhang, S.; Greenfield, M. A.; Mata, A.; Palmer, L. C.; Bitton, R.; Mantei, J. R.; Aparicio, C.; de la Cruz, M. O.; Stupp, S. I. A self-assembly pathway to aligned monodomain gels. *Nat. Mater.* **2010**, *9*, 594–601.

(135) Zhang, X.; Wang, C.; Liao, M.; Dai, L.; Tang, Y.; Zhang, H.; Coates, P.; Sefat, F.; Zheng, L.; Song, J.; et al. Aligned electrospun cellulose scaffolds coated with RHBMP-2 for both in vitro and in vivo bone tissue engineering. *Carbohydr. Polym.* **2019**, *213*, 27–38.



- (136) Yi, B.; Shen, Y.; Tang, H.; Wang, X.; Li, B.; Zhang, Y. Stiffness of aligned fibers regulates the phenotypic expression of vascular smooth muscle cells. *ACS Appl. Mater. Interfaces* **2019**, *11*, 6867–6880.
- (137) Panseri, S.; Cunha, C.; Lowery, J.; Del Carro, U.; Taraballi, F.; Amadio, S.; Vescovi, A.; Gelain, F. Electrospun micro- and nanofiber tubes for functional nervous regeneration in sciatic nerve transections. *BMC Biotechnol.* **2008**, *8*, 39.
- (138) Seonwoo, H.; Shin, B.; Jang, K. J.; Lee, M.; Choo, O. S.; Park, S. B.; Kim, Y. C.; Choi, M. J.; Kim, J.; Garg, P.; et al. Epidermal growth factor-releasing radially aligned electrospun nanofibrous patches for the regeneration of chronic tympanic membrane perforations. *Adv. Healthcare Mater.* **2018**, *8*, No. 1801160.
- (139) Bhattarai, R. S.; Bachu, R. D.; Boddu, S. H. S.; Bhaduri, S. Biomedical applications of electrospun nanofibers: drug and nanoparticle delivery. *Pharmaceutics* **2019**, *11*, 5.
- (140) Raspa, A.; Marchini, A.; Pugliese, R.; Mauri, M.; Maleki, M.; Vasita, R.; Gelain, F. A Biocompatibility study of new nanofibrous scaffolds for nervous system regeneration. *Nanoscale* **2016**, *8*, 253–265.
- (141) Nune, M.; Krishnan, U. M.; Sethuraman, S. Decoration of PLGA electrospun nanofibers with designer self-assembling peptides: a “nano-on-nano” concept. *RSC Adv.* **2015**, *5*, 88748–88757.
- (142) Singh, G.; Bittner, A. M.; Loscher, S.; Malinowski, N.; Kern, K. Electrospinning of diphenylalanine nanotubes. *Adv. Mater.* **2008**, *20*, 2332–2336.
- (143) Tayi, A. S.; Pashuck, E. T.; Newcomb, C. J.; McClendon, M. T.; Stupp, S. I. Electrospinning bioactive supramolecular polymers from water. *Biomacromolecules* **2014**, *15*, 1323–1327.
- (144) Haycock, J. W. 3D cell culture: a review of current approaches and techniques. *Methods Mol. Biol.* **2011**, *695*, 1–15.
- (145) Sanjana, N. E.; Fuller, S. B. A fast flexible ink-jet printing method for patterning dissociated neurons in culture. *J. Neurosci. Methods* **2004**, *136*, 151–163.
- (146) Costa, R. M.; Rauf, S.; Hauser, C. A. E. Towards biologically relevant synthetic designer matrices in 3D bioprinting for tissue engineering and regenerative medicine. *Current opinion in biomedical engineering* **2017**, *2*, 90–98.
- (147) Nolan, M. C.; Fuentes Caparros, A. M.; Dietrich, B.; Barrow, M.; Cross, E. R.; Bleuel, M.; King, S. M.; Adams, D. J. Optimising low molecular weight hydrogels for automated 3D printing. *Soft Matter* **2017**, *13*, 8426–8432.
- (148) Arab, W.; Rauf, S.; Al-Harbi, O.; Hauser, C. A. E. Novel Ultrashort self-assembling peptide bioinks for 3d culture of muscle myoblast cells. *International Journal of Bioprinting* **2018**, *4*, 129.
- (149) Im, H.; Kim, S. H.; Kim, S. H.; Jung, Y. Skin regeneration with a scaffold of predefined shape and bioactive peptide hydrogels. *Tissue Eng., Part A* **2018**, *24*, 1518–1530.
- (150) Li, L.; Li, J.; Guo, J.; Zhang, H.; Zhang, X.; Yin, C.; Wang, L.; Zhu, Y.; Yao, Q. 3D molecularly functionalized cell-free biomimetic scaffolds for osteochondral regeneration. *Adv. Funct. Mater.* **2019**, *29*, 1807356.
- (151) Sundaramurthi, D.; Rauf, S.; Hauser, C. A. E. 3D bioprinting technology for regenerative medicine applications. *Int. J. Bioprint.* **2016**, *2*, 78.
- (152) Raphael, B.; Khalil, T.; Workman, V. L.; Smith, A.; Brown, C. P.; Streuli, C.; Saiani, A.; Domingos, M. 3D cell bioprinting of self-assembling peptide-based hydrogels. *Mater. Lett.* **2017**, *190*, 103–106.
- (153) Matassi, F.; Nistri, L.; Chicon Paez, D.; Innocenti, M. New biomaterials for bone regeneration. *Clin. Cases Miner. Bone Metab.* **2011**, *8*, 21–24.
- (154) Sun, Y.; Li, W.; Wu, X.; Zhang, N.; Zhang, Y.; Ouyang, S.; Song, X.; Fang, X.; Seeram, R.; Xue, W.; et al. Functional self-assembling peptide nanofiber hydrogels designed for nerve degeneration. *ACS Appl. Mater. Interfaces* **2016**, *8*, 2348–2359.
- (155) Zhang, D.; Pekkanen-Mattila, M.; Shahsavani, M.; Falk, A.; Teixeira, A. L.; Herland, A. A 3D alzheimer’s disease culture model and the induction of p21-activated kinase mediated sensing in iPSC derived neurons. *Biomaterials* **2014**, *35*, 1420–1428.
- (156) Zou, Z.; Liu, T.; Li, J.; Li, P.; Ding, Q.; Peng, G.; Zheng, Q.; Zeng, X.; Wu, Y.; Guo, X. Biocompatibility of functionalized designer self-assembling nanofiber scaffolds containing FRM motif for neural stem cells. *J. Biomed. Mater. Res., Part A* **2014**, *102*, 1286.
- (157) Chen, J.; Shi, Z. D.; Ji, X.; Morales, J.; Zhang, J.; Kaur, N.; Wang, S. Enhanced osteogenesis of human mesenchymal stem cells by periodic heat shock in self-assembling peptide hydrogel. *Tissue Eng., Part A* **2013**, *19*, 716–728.
- (158) Miroshnikova, Y. A.; Jorgens, D. M.; Spirio, L.; Auer, M.; Sarang-Sieminski, A. L.; Weaver, V. M. Engineering strategies to recapitulate epithelial morphogenesis within synthetic three-dimensional extracellular matrix with tunable mechanical properties. *Phys. Biol.* **2011**, *8*, 026013.
- (159) Giri, S.; Acikgoz, A.; Pathak, P.; Gutschker, S.; Kursten, A.; Nieber, K.; Bader, A. Three dimensional cultures of rat liver cells using a natural self-assembling nanoscaffold in a clinically relevant bioreactor for bioartificial liver construction. *J. Cell. Physiol.* **2012**, *227*, 313–327.
- (160) Zhao, M.; Song, C.; Zhang, W.; Hou, Y.; Huang, R.; Song, Y.; Xie, W.; Shi, Y.; Song, C. The three-dimensional nanofiber scaffold culture condition improves viability and function of islets. *J. Biomed Mater. Res. A* **2010**, *94*, 667–672.
- (161) Davis, M. E.; Hsieh, P. C.; Takahashi, T.; Song, Q.; Zhang, S.; Kamm, R. D.; Grodzinsky, A. J.; Anversa, P.; Lee, R. T. local myocardial insulin-like growth factor 1 (IGF-1) delivery with biotinylated peptide nanofibers improves cell therapy for myocardial infarction. *Proc. Natl. Acad. Sci. U. S. A.* **2006**, *103*, 8155–8160.
- (162) Hsieh, P. C.; Davis, M. E.; Gannon, J.; MacGillivray, C.; Lee, R. T. Controlled delivery of pdgf-bb for myocardial protection using injectable self-assembling peptide nanofibers. *J. Clin. Invest.* **2005**, *116*, 237–248.
- (163) Lin, Y. D.; Yeh, M. L.; Yang, Y. J.; Tsai, D. C.; Chu, T. Y.; Shih, Y. Y.; Chang, M. Y.; Liu, Y. W.; Tang, A. C.; Chen, T. Y.; et al. Intramyocardial peptide nanofiber injection improves postinfarction ventricular remodeling and efficacy of bone marrow cell therapy in pigs. *Circulation* **2010**, *122*, S132–141.
- (164) Kim, J. H.; Park, Y.; Jung, Y.; Kim, S. H.; Kim, S. H. Combinatorial therapy with three-dimensionally cultured adipose-derived stromal cells and self-assembling peptides to enhance angiogenesis and preserve cardiac function in infarcted hearts. *J. Tissue Eng. Regen. Med.* **2017**, *11*, 2816–2827.
- (165) Segers, V. F.; Tokunou, T.; Higgins, L. J.; MacGillivray, C.; Gannon, J.; Lee, R. T. Local delivery of protease-resistant stromal cell derived factor-1 for stem cell recruitment after myocardial infarction. *Circulation* **2007**, *116*, 1683–1692.
- (166) Castells-Sala, C.; Vallés-Lluch, A.; Soler-Botija, C.; Arnal-Pastor, M.; Martínez-Ramos, C.; Fernandez-Muiños, T.; Mari-Buyé, N.; Lluçia-Valdeperas, A.; Sanchez, B.; Chachques, J. C.; et al. Development of bioactive patch for maintenance of implanted cells at the myocardial infarcted site. *J. Nanomater.* **2015**, *2015*, 1–14.
- (167) Kisiday, J.; Jin, M.; Kurz, B.; Hung, H.; Semino, C.; Zhang, S.; Grodzinsky, A. J. Self-assembling peptide hydrogel fosters chondrocyte extracellular matrix production and cell division: implications for cartilage tissue repair. *Proc. Natl. Acad. Sci. U. S. A.* **2002**, *99*, 9996–10001.
- (168) Lee, H. Y.; Kopesky, P. W.; Plaas, A.; Sandy, J.; Kisiday, J.; Frisbie, D.; Grodzinsky, A. J.; Ortiz, C. Adult bone marrow stromal cell-based tissue-engineered aggrecan exhibits ultrastructure and nano-mechanical properties superior to native cartilage. *Osteoarthritis Cartilage* **2010**, *18*, 1477–1486.
- (169) Miller, R. E.; Grodzinsky, A. J.; Vanderploeg, E. J.; Lee, C.; Ferris, D. J.; Barrett, M. F.; Kisiday, J. D.; Frisbie, D. D. Effect of self-assembling peptide, chondrogenic factors, and bone marrow-derived stromal cells on osteochondral repair. *Osteoarthritis Cartilage* **2010**, *18*, 1608–1619.
- (170) Hong, H. S.; Son, Y. Substance P ameliorates collagen Li-induced arthritis in mice via suppression of the inflammatory response. *Biochem. Biophys. Res. Commun.* **2014**, *453*, 179–184.
- (171) Kim, S. J.; Kim, J. E.; Kim, S. H.; Kim, S. J.; Jeon, S. J.; Kim, S. H.; Jung, Y. Therapeutic effects of neuropeptide substance p coupled with self-assembled peptide nanofibers on the progression of osteoarthritis in a rat model. *Biomaterials* **2016**, *74*, 119–130.

- (172) Ustun, S.; Tombuloglu, A.; Kilinc, M.; Guler, M. O.; Tekinay, A. B. Growth and differentiation of prechondrogenic cells on bioactive self-assembled peptide nanofibers. *Biomacromolecules* **2013**, *14*, 17–26.
- (173) Sun, W.; Xue, B.; Li, Y.; Qin, M.; Wu, J.; Lu, K.; Wu, J.; Cao, Y.; Jiang, Q.; Wang, W. Polymer-supramolecular polymer double-network hydrogel. *Adv. Funct. Mater.* **2016**, *26*, 9044–9052.
- (174) Dufour, A.; Buffier, M.; Vertu-Ciolino, D.; Disant, F.; Mallein-Gerin, F.; Perrier-Groult, E. Combination of bioactive factors and IEIK13 self-assembling peptide hydrogel promotes cartilage matrix production by human nasal chondrocytes. *J. Biomed. Mater. Res., Part A* **2019**, *107*, 893.
- (175) Misawa, H.; Kobayashi, N.; Soto-Gutierrez, A.; Chen, Y.; Yoshida, A.; Rivas-Carrillo, J. D.; Navarro-Alvarez, N.; Tanaka, K.; Miki, A.; Takei, J.; et al. Pura Matrix facilitates bone regeneration in bone defects of calvaria in mice. *Cell Transplant* **2006**, *15*, 903–910.
- (176) Ikeno, M.; Hibi, H.; Kinoshita, K.; Hattori, H.; Ueda, M. Effects of self-assembling peptide hydrogel scaffold on bone regeneration with recombinant human bone morphogenetic protein-2. *Int. J. Oral Maxillofac Implants* **2013**, *28*, No. e283.
- (177) He, B.; Ou, Y.; Chen, S.; Zhao, W.; Zhou, A.; Zhao, J.; Li, H.; Jiang, D.; Zhu, Y. Designer BFGF-incorporated d-form self-assembly peptide nanofiber scaffolds to promote bone repair. *Mater. Sci. Eng., C* **2017**, *74*, 451–458.
- (178) Tsukamoto, J.; Naruse, K.; Nagai, Y.; Kan, S.; Nakamura, N.; Hata, M.; Omi, M.; Hayashi, T.; Kawai, T.; Matsubara, T. Efficacy of a self-assembling peptide hydrogel, SPG-178-gel, for bone regeneration and three-dimensional osteogenic induction of dental pulp stem cells. *Tissue Eng., Part A* **2017**, *23*, 1394–1402.
- (179) Mata, A.; Geng, Y.; Henrikson, K. J.; Aparicio, C.; Stock, S. R.; Satcher, R. L.; Stupp, S. I. Bone regeneration mediated by biomimetic mineralization of a nanofiber matrix. *Biomaterials* **2010**, *31*, 6004–6012.
- (180) Anderson, J. M.; Patterson, J. L.; Vines, J. B.; Javed, A.; Gilbert, S. R.; Jun, H. W. Biphasic peptide amphiphile nanomatrix embedded with hydroxyapatite nanoparticles for stimulated osteo-inductive response. *ACS Nano* **2011**, *5*, 9463–9479.
- (181) Tansik, G.; Kilic, E.; Beter, M.; Demiralp, B.; Kiziltas Sendur, G.; Can, N.; Ozkan, H.; Ergul, E.; Guler, M. O.; Tekinay, A. B. A Glycosaminoglycan mimetic peptide nanofiber gel as an osteoinductive scaffold. *Biomater. Sci.* **2016**, *4*, 1328–1339.
- (182) Gulseren, G.; Yasa, I. C.; Ustahuseyin, O.; Tekin, E. D.; Tekinay, A. B.; Guler, M. O. alkaline phosphatase-mimicking peptide nanofibers for osteogenic differentiation. *Biomacromolecules* **2015**, *16*, 2198–2208.
- (183) Tysseling-Mattiace, V. M.; Sahni, V.; Niece, K. L.; Birch, D.; Czeisler, C.; Fehlings, M. G.; Stupp, S. I.; Kessler, J. A. Self-assembling nanofibers inhibit glial scar formation and promote axon elongation after spinal cord injury. *J. Neurosci.* **2008**, *28*, 3814–3823.
- (184) Tysseling, V. M.; Sahni, V.; Pashuck, E. T.; Birch, D.; Hebert, A.; Czeisler, C.; Stupp, S. I.; Kessler, J. A. Self-assembling peptide amphiphile promotes plasticity of serotonergic fibers following spinal cord injury. *J. Neurosci. Res.* **2010**, *88*, 3161–3170.
- (185) Guo, J.; Su, H.; Zeng, Y.; Liang, Y. X.; Wong, W. M.; Ellis-Behnke, R. G.; So, K. F.; Wu, W. Reknitting the injured spinal cord by self-assembling peptide nanofiber scaffold. *Nanomedicine* **2007**, *3*, 311–321.
- (186) Cigognini, D.; Satta, A.; Colleoni, B.; Silva, D.; Donega, M.; Antonini, S.; Gelain, F. Evaluation of early and late effects into the acute spinal cord injury of an injectable functionalized self-assembling scaffold. *PLoS One* **2011**, *6*, No. e19782.
- (187) Cigognini, D.; Silva, D.; Paloppi, S.; Gelain, F. Evaluation of mechanical properties and therapeutic effect of injectable self-assembling hydrogels for spinal cord injury. *J. Biomed. Nanotechnol.* **2014**, *10*, 309–323.
- (188) Zweckberger, K.; Ahuja, C. S.; Liu, Y.; Wang, J.; Fehlings, M. G. Self-assembling peptides optimize the post-traumatic milieu and synergistically enhance the effects of neural stem cell therapy after cervical spinal cord injury. *Acta Biomater.* **2016**, *42*, 77–89.
- (189) Iwasaki, M.; Wilcox, J. T.; Nishimura, Y.; Zweckberger, K.; Suzuki, H.; Wang, J.; Liu, Y.; Karadimas, S. K.; Fehlings, M. G. Synergistic effects of self-assembling peptide and neural stem/progenitor cells to promote tissue repair and forelimb functional recovery in cervical spinal cord injury. *Biomaterials* **2014**, *35*, 2617–2629.
- (190) Liu, Y.; Ye, H.; Satkunendrarajah, K.; Yao, G. S.; Bayon, Y.; Fehlings, M. G. A self-assembling peptide reduces glial scarring, attenuates post-traumatic inflammation and promotes neurological recovery following spinal cord injury. *Acta Biomater.* **2013**, *9*, 8075–8088.
- (191) Guo, J.; Leung, K. K.; Su, H.; Yuan, Q.; Wang, L.; Chu, T. H.; Zhang, W.; Pu, J. K.; Ng, G. K.; Wong, W. M.; et al. Self-assembling peptide nanofiber scaffold promotes the reconstruction of acutely injured brain. *Nanomedicine* **2009**, *5*, 345–351.
- (192) Sang, L. Y.; Liang, Y. X.; Li, Y.; Wong, W. M.; Tay, D. K.; So, K. F.; Ellis-Behnke, R. G.; Wu, W.; Cheung, R. T. A self-assembling nanomaterial reduces acute brain injury and enhances functional recovery in a rat model of intracerebral hemorrhage. *Nanomedicine* **2015**, *11*, 611–620.
- (193) Francis, N. L.; Bennett, N. K.; Halikere, A.; Pang, Z. P.; Moghe, P. V. Self-assembling peptide nanofiber scaffolds for 3-d reprogramming and transplantation of human pluripotent stem cell-derived neurons. *ACS Biomater. Sci. Eng.* **2016**, *2*, 1030–1038.
- (194) Shi, W.; Huang, C. J.; Xu, X. D.; Jin, G. H.; Huang, R. Q.; Huang, J. F.; Chen, Y. N.; Ju, S. Q.; Wang, Y.; Shi, Y. W.; et al. Transplantation of RADA16-BDNF peptide scaffold with human umbilical cord mesenchymal stem cells forced with CXCR4 and activated astrocytes for repair of traumatic brain injury. *Acta Biomater.* **2016**, *45*, 247–261.
- (195) Jahanbazi Jahan-Abad, A.; Sahab Negah, S.; Hosseini Ravandi, H.; Ghasemi, S.; Borhani-Haghighi, M.; Stummer, W.; Gorji, A.; Khaleghi Ghadiri, M. Human neural stem/progenitor cells derived from epileptic human brain in a self-assembling peptide nanoscaffold improve traumatic brain injury in rats. *Mol. Neurobiol.* **2018**, *55*, 9122–9138.
- (196) Motalleb, R.; Berns, E. J.; Patel, P.; Gold, J.; Stupp, S. I.; Kuhn, H. G. In vivo migration of endogenous brain progenitor cells guided by an injectable peptide amphiphile biomaterial. *J. Tissue Eng. Regen. Med.* **2018**, *12*, No. e2123.
- (197) Angeloni, N. L.; Bond, C. W.; Tang, Y.; Harrington, D. A.; Zhang, S.; Stupp, S. I.; McKenna, K. E.; Podlasek, C. A. Regeneration of the cavernous nerve by sonic hedgehog using aligned peptide amphiphile nanofibers. *Biomaterials* **2011**, *32*, 1091–1101.
- (198) Zhan, X.; Gao, M.; Jiang, Y.; Zhang, W.; Wong, W. M.; Yuan, Q.; Su, H.; Kang, X.; Dai, X.; Zhang, W.; et al. Nanofiber scaffolds facilitate functional regeneration of peripheral nerve injury. *Nanomedicine* **2013**, *9*, 305–315.
- (199) Li, A.; Hokugo, A.; Yalom, A.; Berns, E. J.; Stephanopoulos, N.; McClendon, M. T.; Segovia, L. A.; Spigelman, I.; Stupp, S. I.; Jarrahy, R. A bioengineered peripheral nerve construct using aligned peptide amphiphile nanofibers. *Biomaterials* **2014**, *35*, 8780–8790.
- (200) Nune, M.; Subramanian, A.; Krishnan, U. M.; Kaimal, S. S.; Sethuraman, S. Self-assembling peptide nanostructures on aligned poly(Lactide-co-Glycolide) nanofibers for the functional regeneration of sciatic nerve. *Nanomedicine (London, U. K.)* **2017**, *12*, 219–235.
- (201) Wu, X.; He, L.; Li, W.; Li, H.; Wong, W. M.; Ramakrishna, S.; Wu, W. Functional self-assembling peptide nanofiber hydrogel for peripheral nerve regeneration. *Regen Biomater* **2017**, *4*, 21–30.
- (202) Lu, C.; Wang, Y.; Yang, S.; Wang, C.; Sun, X.; Lu, J.; Yin, H.; Jiang, W.; Meng, H.; Rao, F.; et al. Bioactive self-assembling peptide hydrogels functionalized with brain-derived neurotrophic factor and nerve growth factor mimicking peptides synergistically promote peripheral nerve regeneration. *ACS Biomater. Sci. Eng.* **2018**, *4*, 2994–3005.
- (203) Lu, J.; Sun, X.; Yin, H.; Shen, X.; Yang, S.; Wang, Y.; Jiang, W.; Sun, Y.; Zhao, L.; Sun, X.; et al. A neurotrophic peptide-functionalized self-assembling peptide nanofiber hydrogel enhances rat sciatic nerve regeneration. *Nano Res.* **2018**, *11*, 4599–4613.

- (204) Langer, R. Controlling the movement of molecules. *Q. Rev. Biophys.* **2019**, *52*, e5.
- (205) Nagai, A.; Nagai, Y.; Qu, H.; Zhang, S. Dynamic behaviors of lipid-like self-assembling peptide A<sub>6</sub>D and A<sub>6</sub>K nanotubes. *J. Nanosci. Nanotechnol.* **2007**, *7*, 2246–2252.
- (206) Gelain, F.; Unsworth, L. D.; Zhang, S. Slow and sustained release of active cytokines from self-assembling peptide scaffolds. *J. Controlled Release* **2010**, *145*, 231–239.
- (207) Koutsopoulos, S.; Zhang, S. Two-layered injectable self-assembling peptide scaffold hydrogels for long-term sustained release of human antibodies. *J. Controlled Release* **2012**, *160*, 451–458.
- (208) Di Franco, S.; Amarelli, C.; Montalto, A.; Loforte, A.; Musumeci, F. Biomaterials and heart recovery: cardiac repair, regeneration and healing in the MCS era: a state of the “heart”. *J. Thorac. Dis.* **2018**, *10*, S2346–S2362.
- (209) Zhang, X.; Zhang, W.; Yang, M. Application of hydrogels in cartilage tissue engineering. *Curr. Stem Cell Res. Ther.* **2018**, *13*, 497–516.
- (210) Huang, B. J.; Hu, J. C.; Athanasiou, K. A. Cell-based tissue engineering strategies used in the clinical repair of articular cartilage. *Biomaterials* **2016**, *98*, 1–22.
- (211) Rothdiener, M.; Uynuk-Ool, T.; Sudkamp, N.; Aurich, M.; Grodzinsky, A. J.; Kurz, B.; Rolaufts, B. Human osteoarthritic chondrons outnumber patient- and joint-matched chondrocytes in hydrogel culture-future application in autologous cell-based cartilage repair? *J. Tissue Eng. Regen. Med.* **2018**, *12*, No. e1206.
- (212) Rogers, G. F.; Greene, A. K. Autogenous Bone Graft: Basic science and clinical implications. *J. Craniofac Surg* **2012**, *23*, 323–327.
- (213) Dellavia, C.; Giammattei, M.; Carmagnola, D.; Musto, F.; Canciani, E.; Chiapasco, M. Iliac crest fresh-frozen allografts versus autografts in oral pre-prosthetic bone reconstructive surgery: histologic and histomorphometric study. *Implant Dent* **2016**, *25*, 731–738.
- (214) Amini, A. R.; Laurencin, C. T.; Nukavarapu, S. P. Bone tissue engineering: recent advances and challenges. *Crit. Rev. Biomed. Eng.* **2012**, *40*, 363–408.
- (215) Kretlow, J. D.; Mikos, A. G. Review: Mineralization of synthetic polymer scaffolds for bone tissue engineering. *Tissue Eng.* **2007**, *13*, 927–938.
- (216) Sargeant, T. D.; Guler, M. O.; Oppenheimer, S. M.; Mata, A.; Satcher, R. L.; Dunand, D. C.; Stupp, S. I. Hybrid bone implants: self-assembly of peptide amphiphile nanofibers within porous titanium. *Biomaterials* **2008**, *29*, 161–171.
- (217) Nisbet, D. R.; Wang, T. Y.; Bruggeman, K. F.; Niclis, J. C.; Somaa, F. A.; Penna, V.; Hunt, C. P. J.; Wang, Y.; Kauhausen, J. A.; Williams, R. J.; et al. Shear containment of bdnf within molecular hydrogels promotes human stem cell engraftment and postinfarction remodeling in stroke. *Advanced Biosystems* **2018**, *2*, 1800113.
- (218) Zou, Z.; Zheng, Q.; Wu, Y.; Song, Y.; Wu, B. Growth of rat dorsal root ganglion neurons on a novel self-assembling scaffold containing IKVAV sequence. *Mater. Sci. Eng., C* **2009**, *29*, 2099–2103.
- (219) Adler-Abramovich, L.; Gazit, E. The physical properties of supramolecular peptide assemblies: from building block association to technological applications. *Chem. Soc. Rev.* **2014**, *43*, 6881–6893.
- (220) Reches, M.; Gazit, E. Controlled patterning of aligned self-assembled peptide nanotubes. *Nat. Nanotechnol.* **2006**, *1*, 195–200.
- (221) Das, R.; Kiley, P. J.; Segal, M.; Norville, J.; Yu, A. A.; Wang, L.; Trammell, S. A.; Reddick, L. E.; Kumar, R.; Stellacci, F.; et al. Integration of photosynthetic protein molecular complexes in solid-state electronic devices. *Nano Lett.* **2004**, *4*, 1079–1083.
- (222) Kiley, P.; Zhao, X.; Vaughn, M.; Baldo, M. A.; Bruce, B. D.; Zhang, S. Self-assembling peptide detergents stabilize isolated photosystem i on a dry surface for an extended time. *PLoS Biol.* **2005**, *3*, No. e230.
- (223) Yeh, J. I.; Du, S.; Tortajada, A.; Paulo, J.; Zhang, S. Peptergents: peptide detergents that improve stability and functionality of a membrane protein, glycerol-3-phosphate dehydrogenase. *Biochemistry* **2005**, *44*, 16912–16919.
- (224) Zhao, X.; Nagai, Y.; Reeves, P. J.; Kiley, P.; Khorana, H. G.; Zhang, S. Designer short peptide surfactants stabilize G protein-coupled receptor bovine rhodopsin. *Proc. Natl. Acad. Sci. U. S. A.* **2006**, *103*, 17707–17712.
- (225) Wang, X.; Corin, K.; Baaske, P.; Wienken, C. J.; Jerabek-Willemsen, M.; Duhr, S.; Braun, D.; Zhang, S. Peptide surfactants for cell-free production of functional G protein-coupled receptors. *Proc. Natl. Acad. Sci. U. S. A.* **2011**, *108*, 9049–9054.
- (226) Zhang, S. Lipid-like self-assembling peptides. *Acc. Chem. Res.* **2012**, *45*, 2142–2150.
- (227) Koutsopoulos, S.; Kaiser, L.; Eriksson, H. M.; Zhang, S. Designer peptide surfactants stabilize diverse functional membrane proteins. *Chem. Soc. Rev.* **2012**, *41*, 1721–1728.
- (228) Wu, Y.; Norberg, P. K.; Reap, E. A.; Congdon, K. L.; Fries, C. N.; Kelly, S. H.; Sampson, J. H.; Conticello, V. P.; Collier, J. H. A supramolecular vaccine platform based on a-helical peptide nanofibers. *ACS Biomater. Sci. Eng.* **2017**, *3* (12), 3128–3132.
- (229) Luo, Z.; Wang, S.; Zhang, S. Fabrication of self-assembling D-form peptide nanofiber scaffold d-EAK16 for rapid hemostasis. *Biomaterials* **2011**, *32*, 2013–2020.